Atmos. Chem. Phys. Discuss., https://doi.org/10.5194/acp-2018-949
Manuscript under review for journal Atmos. Chem. Phys.
Discussion started: 3 January 2019

Atmospheric Chemistry and Physics Discussions

Aerosol radiative effects with MACv2

Stefan Kinne[1]

[1]Max-Planck Institute for Meteorology, Hamburg, 20146, Germany

Correspondence to: Stefan Kinne (Stefan.Kinne@mpimet.mpg.de)

Abstract. Monthly global maps for aerosol properties of the MACv2 climatology are applied in an off-line radiative transfer model to determine aerosol radiative effects. For details beyond global averages in most cases global maps are presented to visualize regional and seasonal details. Aside from the direct radiative (aerosol presence) effect, including those for aerosol components as extracted from MACv2 aerosol optics, also the major aerosol indirect radiative effect is covered. Hereby, the impact of smaller drops in water clouds due to added anthropogenic aerosol was simulated by applying a satellite retrieval based fit from locally associations between aerosol and drop concentrations over oceans. Present-day anthropogenic aerosols of MACv2 - on a global average basis - reduce the radiative net-fluxes at the top of the atmosphere (TOA) by -1.0 W/m2 and at the surface by -2.1 W/m2. Direct cooling contributions are only about half of indirect contributions (-.35 vs -.65) at TOA, but about twice at the surface (-1.45 vs -.65), as solar absorption of the direct effect warms the atmosphere by +1.1 W/m2. Natural aerosols are on average less absorbing (for a relatively larger solar TOA cooling) and larger in size (now contributing with IR greenhouse warming). Thus, average TOA direct forcing efficiencies for total and anthropogenic aerosol happen to be similar: -11 W/m2/AOD at all-sky and -24 W/m2/AOD at clear-sky conditions. The present-day direct impact by all soot (BC) is globally averaged +0.55W/m2 and at least half of it should be attributed to anthropogenic sources. Hereby any accuracy of anthropogenic impacts, not just for soot, suffers from the limited access to a pre-industrial reference. Anthropogenic uncertainty has a particular strong impact on aerosol indirect effects, which dominate the (TOA) forcing. Accounting for uncertainties in the anthropogenic definition, present-day aerosol forcing is estimated to stay within the -0.7 to -1.6 W/m2 range, with a best estimate at -1 W/m2. Calculations with model predicted temporal changes to anthropogenic AOD indicate that qualitatively the anthropogenic aerosol forcing has not changed much over the last decades and is not likely to increase over the next decades, despite strong regional shifts. These regional shifts explain most solar insolation (brightening or dimming) trends that have been observed by ground-based radiation data.

1 Introduction

Atmospheric aerosol modulates the radiative energy budget directly (by the aerosol presence) and indirectly (by modifying the properties of clouds). Such impacts are of interest for climate change predictions, because part of today's

atmospheric aerosol is anthropogenic. A quantification of aerosol impacts on global scales, however, is difficult, as tropospheric aerosol is highly variable in space and time and as the needed pre-industrial reference for anthropogenic impacts is highly uncertain. The determination of aerosol impacts requires two simulations: one with aerosol and one with less or no aerosol. Usually complex 'bottom-up' simulations with global models are applied, in which emissions of different aerosol sources are chemically and/or cloud processed, mixed, transported and removed. With further assumptions to size and water uptake associated aerosol radiative properties are determined so that eventually the radiative impact can be calculated with broadband radiative transfer methods. This process involves many uncertainties and becomes even more uncertain as natural variability comes into play with an added requirement to account for feedbacks and delayed or spatially detached responses. Fortunately, feedbacks can be considered as secondary (*Fiedler et al. 2017*) so that dual-call radiative transfer simulations seem sufficient. In these dual-call simulations noise from natural variability is avoided, as only specific properties to aerosol (for direct impacts) and/or to aerosol modified clouds (for total / indirect impacts) in an otherwise identical environment are varied. Here a radiative transfer dual-call approach is applied, which starts with aerosol optical properties rather than with emissions. Thus, time-consuming aerosol processing and potential uncertainties from aerosol processing are avoided. This approach is referred to as 'top-down', as aerosol microphysical and component details in reverse processing can be extracted from aerosol optics. The MACv2 aerosol climatology (*Kinne, 2018*) provides the needed global (monthly, 1x1deg gridded) maps for spectrally resolved aerosol single scattering properties of total and anthropogenic aerosol as a function of time. Still, to simulate aerosol radiative impacts also environmental properties are influential. Thus, after introducing the assumed MACv2 properties, also the environmental properties and the applied radiative transfer scheme are outlined, before impact results are presented for total and anthropogenic aerosol, also as a function of time.

2 MACv2 Aerosol Properties

The **M**ax Planck institute **A**erosol **C**limatology (MAC) in its second version (*Kinne, 2018*) defines spectrally resolved monthly global fields for aerosol radiative properties with global coverage (at a 1x1 degree lat/lon spatial resolution). Annual averages of defining MACv2 properties are shown in Figure 1.

Atmos. Chem. Phys. Discuss., https://doi.org/10.5194/acp-2018-949
Manuscript under review for journal Atmos. Chem. Phys.
Discussion started: 3 January 2019

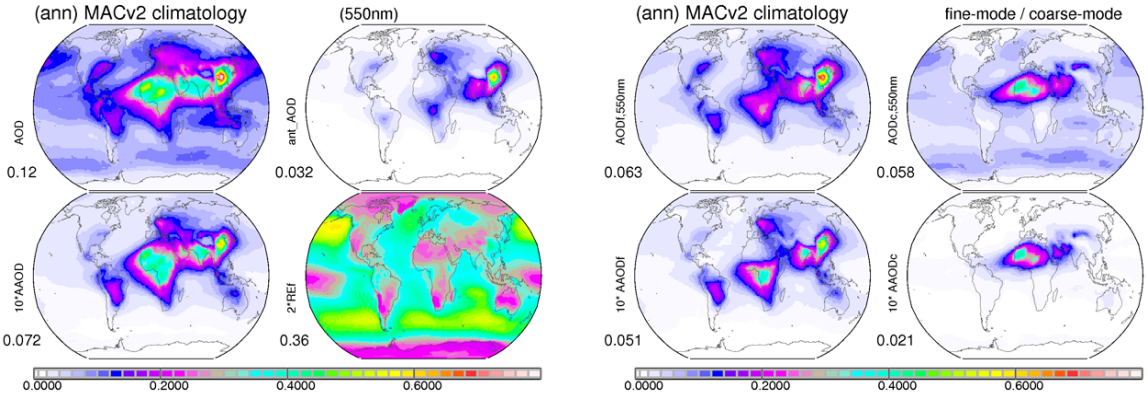

Figure 1. *annual average maps of the MACv2 aerosol climatology. Global distributions are presented for present day column properties of aerosol amount (AOD), absorption (AAOD*10), anthropogenic AOD and fine-mode size (REf*2). Also presented are mid-visible AOD and 10*AAOD maps split into fine-mode (radii <0.5um) and coarse mode (radii >0.5um) contributions. Values below labels show global averages.*

These global fields are the result of a data merging process for mid-visible aerosol optical properties. Monthly maps from global modeling were adjusted by region with monthly statistics from ground based solar photometry observations. Applied solar photometry monthly statistics are sun- and sky- samples by CIMEL instruments of the AERONET network (*Holben et al. 2001, Dubovik et al, 2002*) and sun-samples by handheld MICROTOPS instruments of the Marine Aerosol Network, MAN (*Smirnov et al., 2009*). The needed spatial context (on regional scales) is provided by a monthly ensemble median of 14 different AeroCom (phase1) models (*Kinne et al., 2006*). The needed spectrally varying single scattering properties for broadband radiative transfer simulation are set by local mixtures of spectrally (via refractive index and size) defined aerosol components, whose mixtures are consistent with MACv2 size-mode separated mid-visible properties for aerosol optical depth (AOD, for column amount) and absorption aerosol optical depth (AAOD, for column absorption) and the fine-mode effective radius (REf). Annual average spatial distributions to these properties are illustrated in Figure 1. Figure 1 also presents the MACv2 estimate for the present-day mid-visible anthropogenic AOD. In MACv2 anthropogenic AOD is only allowed to add to smaller fine-mode (radii>0.5um) aerosol sizes. It is defined by applying to the MACv2 fine-mode AOD (AODf) a scaling factor [=(AODf,pd -AOD,pi) /AOD,pd)] from global modeling with IPCC5 present-day (pd) and pre-industrial (pi) emissions (*Larmarque et al, 2010*). Seasonal maps of single scattering properties (at 550nm) for total and anthropogenic aerosol are presented in Figure 2. Global averages are compared in Table 1, also in other spectral regions.

Atmos. Chem. Phys. Discuss., https://doi.org/10.5194/acp-2018-949
Manuscript under review for journal Atmos. Chem. Phys.
Discussion started: 3 January 2019

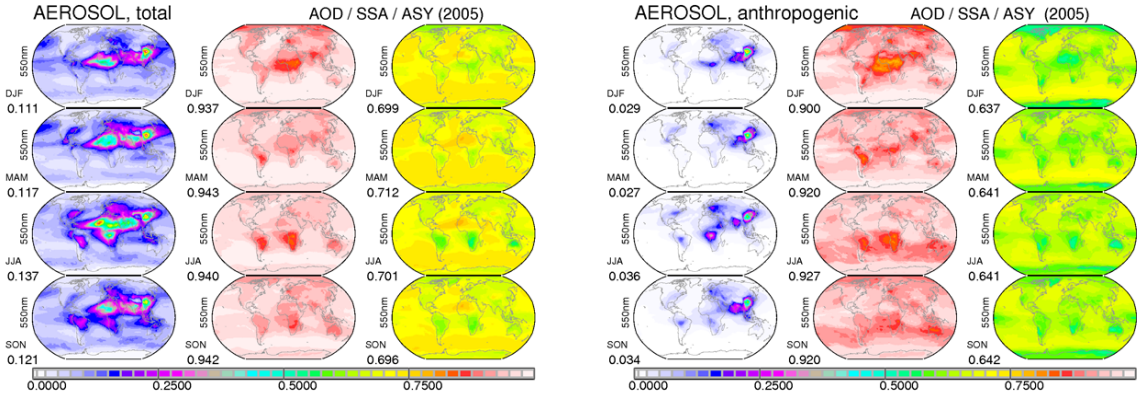

Figure 2. *seasonal maps of MACv2 associated present-day mid-visible single scattering properties (AOD, SSA, ASY) for all aerosol (left block) and for anthropogenic aerosol (right block). Global averages for each season are indicated below the labels.*

Table 1 *global annual average aerosol radiative properties for present-day (tropospheric) aerosol*

	AOD				SSA			ASY		
λ(μm)	***total***	*coarse*	*fine*	*anthr**	*total*	*coarse*	*fine*	*total*	*coarse*	*fine*
.45	**0.144**	0.058	0.087	0.043	0.902	0.905	0.900	0.718	0.789	0.670
.55	**0.122**	0.058	0.063	0.032	0.941	0.964	0.919	0.702	0.767	0.639
1.0	**0.081**	0.062	0.019	0.009	0.956	0.982	0.870	0.693	0.736	0.533
10	**0.049**	0.049			0.580	0.560		0.605	0.605	

** anthropogenic SSA and ASY are that of the fine-mode*

Other important MACv2 aerosol properties are AOD vertical distributions, separately for fine-mode and coarse-mode sizes, and changes in anthropogenic AOD over time, as illustrated in Figure 3.

Atmos. Chem. Phys. Discuss., https://doi.org/10.5194/acp-2018-949
Manuscript under review for journal Atmos. Chem. Phys.
Discussion started: 3 January 2019

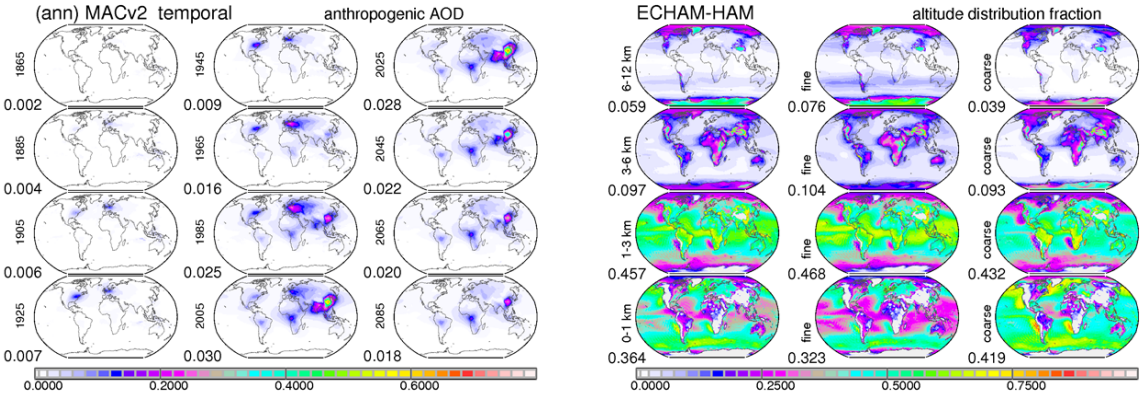

Figure 3 *annual maps for anthropogenic AOD (550nm) for different years from 1865 to 2085 (left block) and for fractional contributions of total, fine-mode and coarse mode AOD (right block) for four altitude regimes (0-1, 1-3, 3-6, >6km above sea-level). Values below the label indicate global averages.*

The temporal change in anthropogenic AOD as in MACv1 (*Kinne et al, 2013*) is based on global model simulations with temporally changing emissions. Hereby ratios of simulated anthropogenic AODf for years of choice with respect to the simulated anthropogenic AODf with present-day emissions are scaled to the present-day anthropogenic AOD of MACv2. The resulting anthropogenic AOD maps for selected historic and future years in Figure 3 display globally highly uneven distributions with larger maxima over urban-industrial regions of the northern hemisphere. Despite strong regional shifts in regional maxima (from US and Europe to SE Asia) changes to the annual global averages over the last three decades are relatively small and are presently near a global average maximum.

The vertical distribution (*Kinne 2018*) is based on multi-annual simulations by applying present-day emissions in a global model. Based on resulting vertical distributions for fine-mode AOD (AODf) and coarse-mode AOD (AODc) fractional scaling factors are applied separately to the AODf and AODc data of the MACv2 climatology for all atmospheric layers of the radiative transfer model. With separate AOD altitude assignments by size-mode, further vertical dependencies to SSA or ASY seem secondary and are not considered. For anthropogenic aerosol, which in MACv2 only modifies the fine-mode AOD (changes to SSA and ASY are considered as secondary) only the AODf scaling is applied.

3 Environmental Properties

The environmental properties in radiative transfer simulations are represented by monthly averages to describe seasonal variations in solar insolation, surface properties and cloud properties - as in MACv1 (*Kinne et al., 2013*). For solar insolation the monthly mean latitude of the sun is prescribed. Surface temperatures of the GISS global model are applied and

Atmos. Chem. Phys. Discuss., https://doi.org/10.5194/acp-2018-949
Manuscript under review for journal Atmos. Chem. Phys.
Discussion started: 3 January 2019

a surface infrared emittance of 0.96 is assumed. Surface albedo data over land are based on MODIS sensor data for the UV/VIS and n-IR spectral regions (*Schaaf et al., 2002*) and over oceans a solar elevation dependence (*Taylor et al., 1996*) is applied. For clouds multi-annual ISSCP data (*Rossow et al., 1993*) define scene optical depth and cover at low, mid and high altitudes. Seasonal means of applied MODIS and ISCCP data are shown in Figure 4.

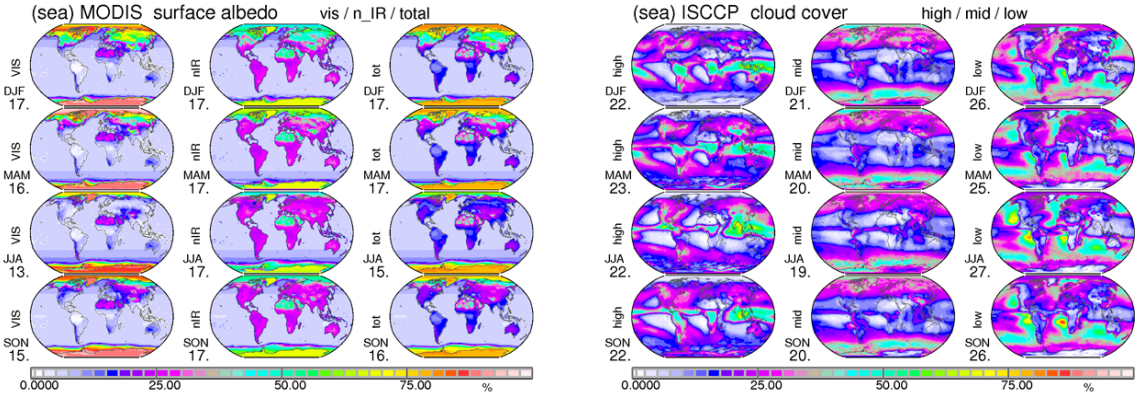

Figure 4 *Seasonal averages for applied environmental properties to (1) solar surface albedo (left block) for the UV/VIS, the near-IR and the total spectral range based on MODIS satellite sensor data and (2) ISCCP based cloud cover (right block) for high (<440hPa), mid (440-680hPa) and low (>680hPa) altitudes.*

4 Radiative Transfer Method

The atmospheric radiative transfer simulations apply a two stream radiative transfer model (*Meador and Weaver, 1980*). Spectral variability is captured by eight solar and twelve infrared bands with a total of 120 exponential terms to represent atmospheric trace-gas absorption. Vertical variability of the atmosphere is represented by 20 plane parallel homogenous layers and atmospheric state and trace-gas properties are defined via standard atmospheres (*Mc Clatchey et al, 1972*). Independent simulations at each (of the 64800) grid locations are performed with monthly averages. Hereby, daily average solar radiative effects are based weighted individual simulations at nine different solar zenith angles. And simulations with (ISCCP) clouds always involve simulations at all eight possible permutations for high-, mid- and low-altitude cloud combinations, assuming random overlap for satellite view corrected local cloud cover data in the three altitude regimes.

Radiative impacts in the atmosphere are derived from ‘dual-call’ applications, where differences are explored between a specifically modified configuration and the standard configuration. Here, dual-call applications investigate radiative impacts of (1) an extra aerosol presence (direct effect - with an added focus on individual aerosol components), (2) reduced water droplet radii due to extra aerosol (indirect effect) and (3) the combination of both effects. Of particular interest

are resulting changes to broadband solar and infrared radiative net-fluxes (1) at the top of the atmosphere (TOA) for the overall climate impact, (2) at the surface for impacts on surface processes and (3) within the atmosphere for impact on dynamics (derived from the difference of TOA effect minus surface effect).

Dual-call simulations ignore feedbacks, as they could be considered in complex Earth-System models (ESM). However, long-term ESM simulations have indicated that these feedbacks are relatively small - on the order of 10%. Moreover, dual-calls offer much more certainty, as internal variability of independent ESM simulations is avoided (*Fielder et al, 2018*).

5 Direct Radiative Effects

Aerosol direct radiative effects are changes to the atmospheric energy distribution from the aerosol (or the extra aerosol) presence. These effects are quantified by the difference of one simulation with all aerosol and one simulation with no (for total effects) or partially removed aerosol (as anthropogenic or individual MACv2 defined components). Annual average maps of present day direct aerosol radiative effects are summarized in Figure 5 for cloud-free conditions (clear-sky, 'clr') and with tropospheric clouds (all-sky, 'all') - for both total and anthropogenic aerosol at TOA and surface.

Atmos. Chem. Phys. Discuss., https://doi.org/10.5194/acp-2018-949
Manuscript under review for journal Atmos. Chem. Phys.
Discussion started: 3 January 2019

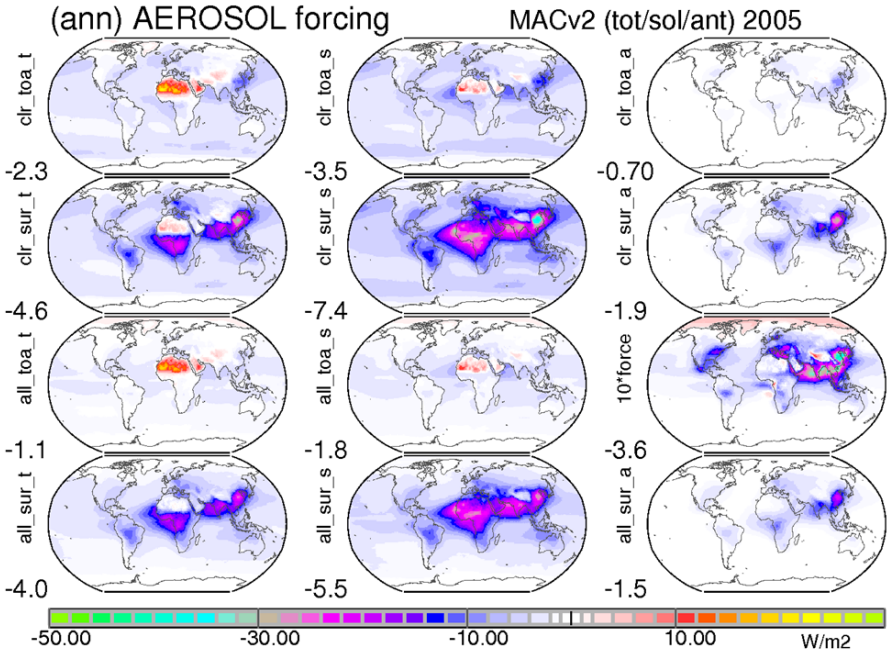

Figure 5 *Annual maps for direct radiative effects of present-day total aerosol (left column), its solar effect (center column) and of present-day anthropogenic aerosol. Clear-sky effects are presented in the upper two rows: at the TOA (row 1) and at the surface (row2). All-sky effects (with ISCCP clouds) are presented in the lower two rows: at the TOA (row 3) and at the surface (row 4). Note, values in the annual map for present day anthropogenic direct forcing (column 3, row3) are multiplied by a factor 10. Blue colors indicate radiative netflux losses or a cooling, and red colors indicate radiative netflux gains or a warming. Values below the labels indicate global averages.*

The aerosol direct radiative effects are unevenly distributed over the globe. In Figure 5 blue colors (or negative values) indicate a tendency to cool. These are cases when the netflux ('downward-flux' minus 'upward-flux') is reduced: at the TOA via increased radiative losses to space or at the surface via reduced radiation reaching the surface. In contrast, red colors (or positive values) in Figure 5 indicate a tendency to warm. Aerosol direct radiative effects at the surface are more negative than at the top of the atmosphere (TOA) due to added losses by solar absorption in the atmosphere. And radiative effects at clear-sky conditions are more negative than at all-sky conditions, mainly as clouds above aerosol prevent aerosol interactions with solar radiation. Another contribution to lower all-sky effects at the TOA is an absorbing aerosol dimming of solar reflection by clouds or bright surfaces below the aerosol. Thus, less negative TOA responses even yield over a few regions a TOA solar warming. Globally averaged, however, present-day aerosol direct radiative effects cause a (solar) cooling - even at all-sky conditions and even at the TOA.

Atmos. Chem. Phys. Discuss., https://doi.org/10.5194/acp-2018-949
Manuscript under review for journal Atmos. Chem. Phys.
Discussion started: 3 January 2019

Atmospheric Chemistry and Physics Discussions

For present-day total aerosol on average ca 35% of the solar losses are compensated by IR gains. Almost entirely caused by elevated super-micrometer mineral dust sizes this IR warming is so large over continents that mineral dust is almost climate neutral, as later illustrated in Appendix E. Anthropogenic aerosol in MACv2 only allows sub-micrometer size contributions, so only solar radiative impacts matter. For present-day anthropogenic aerosol the climate change relevant aerosol direct forcing (the direct radiative effects by anthropogenic aerosol at all-sky conditions at TOA) yields a cooling near -0.35W/m2. This direct forcing signal is on average more than a magnitude smaller than ground detectable solar radiation reductions or satellite detectable planetary albedo increases over oceans. More details on seasonal variability, present-day direct aerosol monthly forcing distributions are presented in Figure 6.

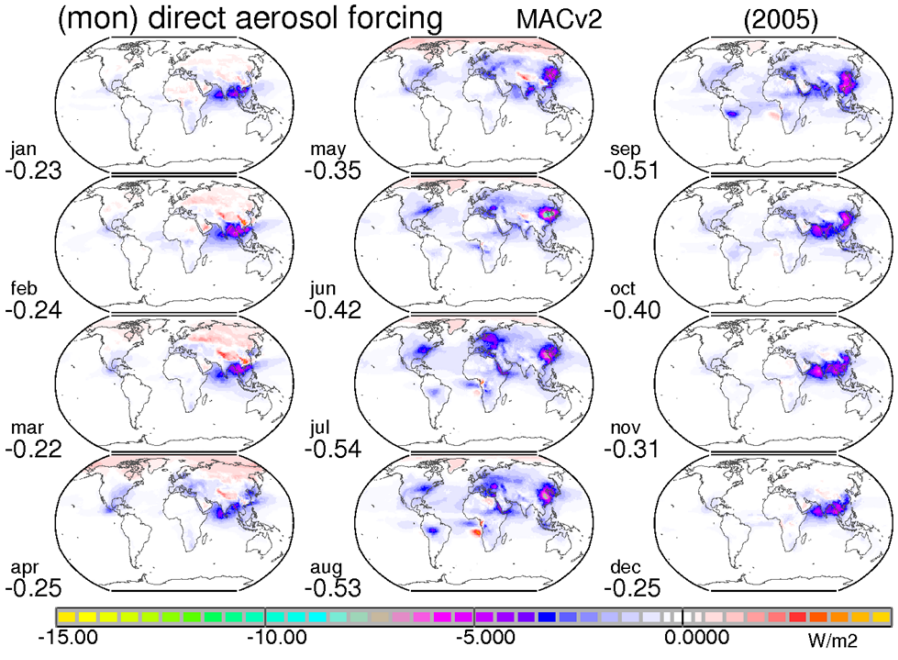

Figure 6 *Monthly maps for present-day aerosol direct forcing with MACv2 aerosol properties*

On a global average basis the present-day aerosol direct forcing causes a cooling during the entire year. The cooling is strongest during the northern hemispheric summer, mainly due to more sun-hours and higher AOD values, in part caused by increased water uptake at warmer temperatures. And the cooling is smallest during the northern hemispheric spring, in part also due to a slight warming over snow covered regions (e.g. Asia, Arctic). Also of note is the regional warming over

Atmos. Chem. Phys. Discuss., https://doi.org/10.5194/acp-2018-949
Manuscript under review for journal Atmos. Chem. Phys.
Discussion started: 3 January 2019

Atmospheric Chemistry and Physics Discussions

the SE Atlantic during August, due the dimming of solar reflection of lower altitude clouds by absorbing aerosol from biomass burning. The spatial distribution of the aerosol direct forcing illustrates a dominance of regional contributions with maxima in excess of -5W/m2 over southern and eastern Asia. More details on present-day direct radiative effects are provided by investigating contributions by the (sub-micrometer) fine-mode sizes in Figure 7 and by (super-micrometer) coarse-mode size in Figure 8.

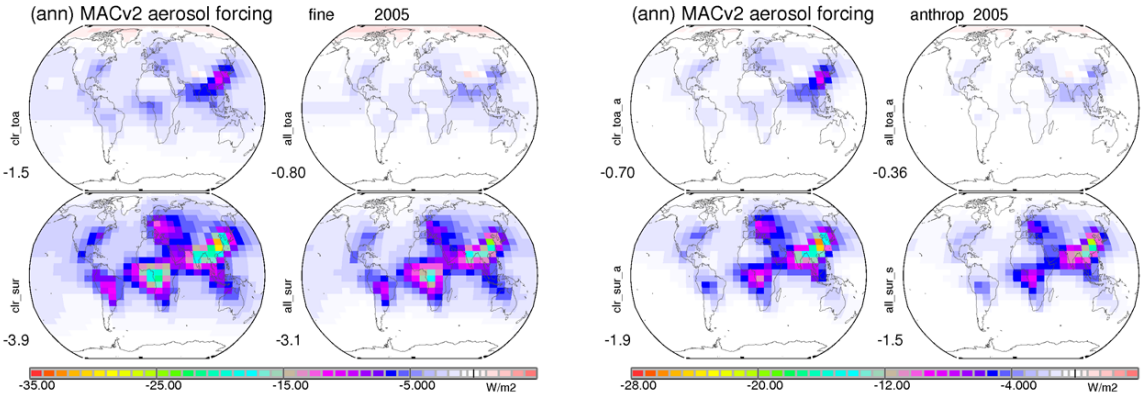

Figure 7 *Annual maps for present-day fine-mode aerosol direct (solar) radiative effects at TOA (top) and surface (bottom) for clear-sky (left) and all-sky (right) conditions. Blue colors indicate a cooling and red colors a warming. Today's fine-mode effects (left block) are compared to today's anthropogenic effects (right block). Values below the labels indicate global averages.*

Fine-mode and coarse mode radiative effects differ is their regional contributions. On a global average basis, fine-mode contributions to (climate) cooling are stronger, despite stronger solar fine-mode absorption. This is in part related that coarse-mode aerosol is large enough in size to interact with longwave radiation and with significant IR warming contributions via elevated mineral dust over northern Africa, Arabia and Asia. The separation of coarse mode aerosol direct radiative effects at TOA and surface in Figure 8 demonstrate partially compensating solar cooling and IR warming effects. Over the Sahara region already the solar TOA effect is warming and in that case the IR warming adds to it.

Also shown in Figure 7 and 8 are size-mode associated aerosol direct radiative effects attributed to anthropogenic sources. For the fine-mode about 50% of present-day fine-mode radiative effects are anthropogenic (thus half of the fine-mode was already contributing at pre-industrial times). Potential coarse mode anthropogenic contributions to the present-day coarse-mode radiative effects are uncertain but probably small. The illustrated anthropogenic coarse-mode forcing of +0.02 W/m2 applies an anthropogenic mineral dust fraction estimate of a satellite sensor data analysis (*P. Ginoux, personal communication*). This is negligible in comparison to the anthropogenic fine-mode impact of -0.36W/m2.

Atmos. Chem. Phys. Discuss., https://doi.org/10.5194/acp-2018-949
Manuscript under review for journal Atmos. Chem. Phys.
Discussion started: 3 January 2019

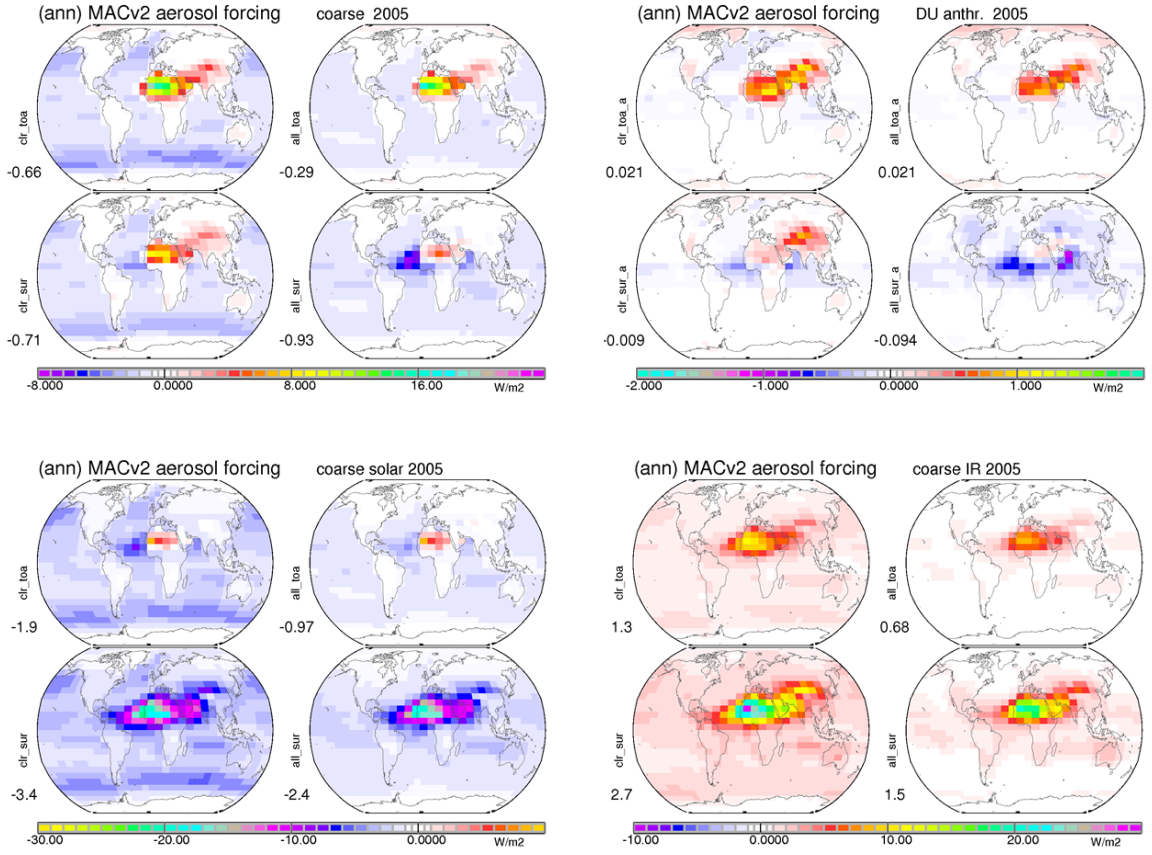

Figure 8 *Annual maps for the coarse-mode aerosol direct radiative effects at TOA (top) and surface (bottom) for clear-sky (left) and all-sky (right) conditions. Coarse-mode effects (top, left block) are compared to potential anthropogenic contributions (top, right block) which for better viewing were multiplied by a factor of 10). Blue colors indicate a cooling and red colors a warming. In addition, solar (bottom, left block) and IR contributions (bottom, right block) to the coarse-mode aerosol direct radiative effects are presented. Note the different scales. Values below the labels indicate global averages.*

With the AOD attributions in MACv2 into radiatively defined components via their mid-visible absorption properties (*Kinne, 2018*) and via the anthropogenic definition in MACv2, direct aerosol radiative effects of components and their anthropogenic contributions could be determined. Note, that the sub-sequent absorption categories refer to the mid-visible spectral region. For the aerosol fine-mode, direct radiative effects are contributed by non-absorbing aerosol represented by sulfate (SU), by weakly absorbing organic matter (OC) and by strongly absorbing soot (BC). Also the combined carbon (CA = OC+BC) effect is examined to estimate soot co-emitter effects. For the coarse-mode, direct

Atmos. Chem. Phys. Discuss., https://doi.org/10.5194/acp-2018-949
Manuscript under review for journal Atmos. Chem. Phys.
Discussion started: 3 January 2019

Atmospheric Chemistry and Physics Discussions

radiative effects are contributed by non-absorbing seasalt (SS) and weakly absorbing mineral dust (DU). Hereby larger coarse-mode absorption translates into larger mineral dust sizes. Annual maps for present-day direct radiative component effects at TOA at clear-sky and (climate impact relevant) all-sky conditions are shown in Figure 9. More details on component direct radiative effects are presented in Appendix E.

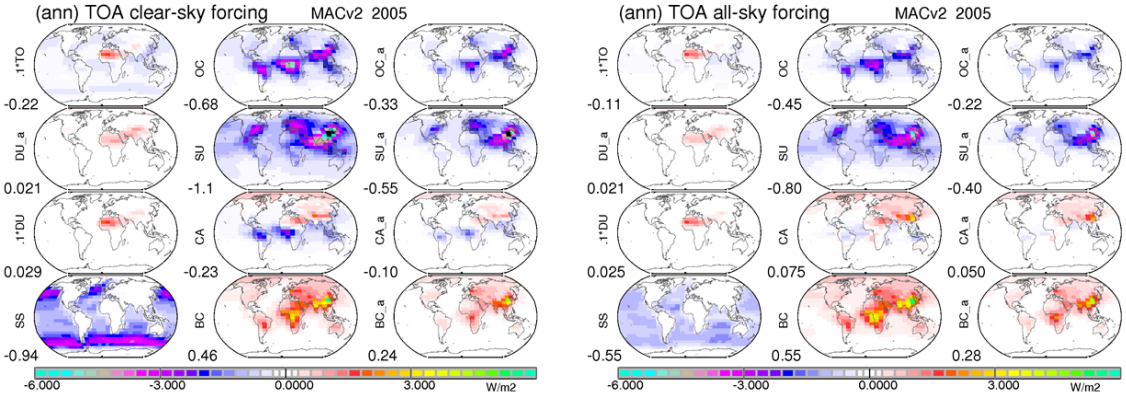

Figure 9 *Annual maps for today's direct forcing at TOA at clear-sky (left block) and at all-sky conditions (right block) by total aerosol (TO, divided by 10 to fit common scale) and by coarse-mode components of anthropogenic dust (DU_a), dust (DU, divided by 10 to fit common scale) and sea-salt (SS) in the left column, by fine-mode components of non-absorbing sulfate (SU), of weakly absorbing organic matter (OC), of strong absorbing soot (BC) and of the combined carbon (CA=OC+BC) component in the center column and by the anthropogenic contributions of the fine-mode components in the right column. Global averages for the annual direct aerosol component TOA effects are presented below the labels.*

The radiative TOA direct radiative effects of individual components are quite diverse. Climate cooling by sulfate (SU), sea-salt (SS), organic matter (OC) and dust (DU-o) over oceans is on average stronger than climate warming by soot (BC) and dust (DU-c) over continents. As MACv2 only considers anthropogenic contributions to the fine-mode, investigations of anthropogenic impacts can be reduced to cooling by non-absorbing SU and OC and warming by BC. The combined carbon (CA) approximates the impacts of co-emitted gases that quickly condensate on existing particles (including soot) to increase scattering on existing particles (also in the context of an upper limit near 2 for a soot absorption increase via a scattering shell). The combined CA forcing is near neutral (+0.05 W/m2) and would suggest that only change in fine-mode non-absorbing AOD should be considered to quantify aerosol direct forcing.

The CA near neutral response, however, only applies, if the BC anthropogenic fraction is that of the fine-mode AOD fraction. With a higher soot (BC) anthropogenic fraction (especially near pollution regions), as assumed in the BC assessment (*Bond et al., 2013*), the present-day BC forcing increases to +0.44 W/m2 as shown in Appendix E. This added BC warming would increases present-day CA warming to +0.20 W/m2 and at the same tome would reduce the present day

total direct aerosol forcing to -0.20 W/m2. Under the aspect, however, that this anthropogenic fraction is linked to a year 1750 reference, whereas a year 1850 reference contains already pre-existing BC over Europe and the US such an increase to the BC anthropogenic impact probably should be, if at all, only considered in part.

The consideration of co-emitted gases soot (BC) removal processes may not have the often attributed potential for short term climate warming mitigations. Thus, the singled out present-day warming +0.55 W/m2 for all soot (BC) with estimated anthropogenic contributions between +0.28 to +0.35 W/m2 is deceiving as co-emitters also have to considered in removal processes.

Annual averages of MACv2 aerosol associated direct radiative effects for present day atmospheric conditions are summarized in Tables 2 and 3. Table 2 compares radiative effects at TOA, atmosphere and surface for all aerosol, fine-mode only aerosol, coarse-mode only aerosol and individual aerosol components. Table 3 compares solar and infrared contributions of components with non-negligible infrared impacts. Table 2 associated global maps for component radiative effects are presented in Appendix D.

Table 2 *annual average MACv2 climatology associated aerosol radiative effects for today's tropospheric aerosol at the top of the atmosphere (TOA), at the surface and (by difference) for the atmosphere. Aside for total aerosol (in row 1) also effects of components and if applicable their anthropogenic contributions are indicated. Considered fine-mode components are sulfate (SU), organic carbon (OC), soot (BC) and the combined carbon (OC+BC). Considered coarse-mode components are sea-salt (SS) and dust (DU).*

direct effect (W/m2)	**TOA**				**ATMOSPHERE**				**SURFACE**			
	total		*anthr*		*total*		*anthr*		*total*		*anthr*	
	all	***clear***	***all***	***clear***	***all***	***clear***	***all***	***clear***	***all***	***clear***	***all***	***clear***
total	**-1.1**	**-2.2**			**+2.9**	**+2.3**			**-4.0**	**-4.5**		
fine	-0.80	-1.5	**-0.36**	**-0.70**	+2.3	+2.4	**+1.1**	**+1.2**	-3.1	-3.9	**-1.5**	**-1.9**
- SU	-0.83	-1.2	-0.41	-0.58	+0.02	+0.03	+0.01	+0.01	-0.85	-1.2	-0.42	-0.59
- CA	+0.08	-0.23	+0.05	-0.10	+2.0	+2.2	+1.0	+1.1	-2.1	-2.5	-1.0	-1.2
- OC	-0.45	-0.68	-0.22	-0.33	+0.48	+0.52	+0.23	+0.25	-0.93	-1.2	-0.45	-0.57
- BC	+0.55	+0.46	+0.28	+0.24	+1.7	+1.8	+0.89	+0.93	-1.2	-1.4	-0.61	-0.69
- BC*			+0.44	+0.37			+1.4	+1.5			-0.97	-1.1
coarse	-0.29	-0.66			+0.64	+0.05			-0.93	-0.71		
- SS	-0.55	-0.94			+0.00	-0.11			-0.55	-0.83		
- DU	+0.25	+0.29	+0.02	+0.02	+0.63	+0.17	+0.11	+0.03	-0.38	+0.12	-0.09	-0.01

**using AeroCom 1 of MACv1 (rather than AeroCom 2 of MACv2) anthropogenic fine-mode fractions*

Atmos. Chem. Phys. Discuss., https://doi.org/10.5194/acp-2018-949
Manuscript under review for journal Atmos. Chem. Phys.
Discussion started: 3 January 2019

Atmospheric Chemistry and Physics Discussions

Table 3 *annual average MACv2 climatology associated aerosol radiative effects for today's tropospheric aerosol at the top of the atmosphere (TOA) and at the surface, by separating solar and IR contributions. Aside for the total aerosol (in row1) also effects are presented for components with an IR impact, such as seasalt (SS), dust (DU) and anthropogenic dust (aDU).*

direct effect (W/m2)	**TOA**						**SURFACE**					
	all-sky			***clear-sky***			***all-sky***			***clear-sky***		
		solar	IR		solar	IR		solar	IR		solar	IR
total	-1.1	-1.8	+0.71	-2.2	-3.5	+1.3	-4.0	-5.5	+1.5	-4.5	-7.3	+2.8
coarse	-.029	-0.97	+0.68	-0.66	-1.9	+1.3	-0.93	-2.4	+1.5	-0.71	-3.4	+2.7
- SS	-0.55	-0.72	+0.17	-0.94	-1.4	+0.42	-0.55	-0.77	+0.22	-0.83	-1.4	+0.58
- DU	+0.25	-0.25	+0.50	+0.29	-0.55	+0.84	-0.38	-1.6	+1.2	+0.12	-2.0	+2.1
- aDU	+0.02	-0.06	+0.08	+0.02	-0.13	+0.15	-0.09	-0.30	+0.20	-0.01	-0.37	+0.36

6 Direct Forcing Efficiencies

Forcing efficiencies offer a shortcut to radiative effects without actually performing radiative transfer simulations. In that context also influences by environmental properties (such as surface albedo, solar insolation and even clouds) are already included. A satellite retrieved AOD value or an anthropogenic AOD enhancement then can be quickly associated with a radiative effect simply by multiplying with the appropriate forcing efficiency. In such applications even information on the likely aerosol composition is included. Applying environmental assumptions and MACv2 aerosol properties in radiative transfer off-line simulations, aerosol direct forcing efficiencies are presented with respect to the mid-visible AOD (as often used in conjunction with satellite retrievals and global modeling). Annual maps for forcing efficiencies per unit AOD for total and anthropogenic aerosol are presented in Figure 10. Seasonal variations of these global averages are small, as shown in Appendix D.

Atmos. Chem. Phys. Discuss., https://doi.org/10.5194/acp-2018-949
Manuscript under review for journal Atmos. Chem. Phys.
Discussion started: 3 January 2019

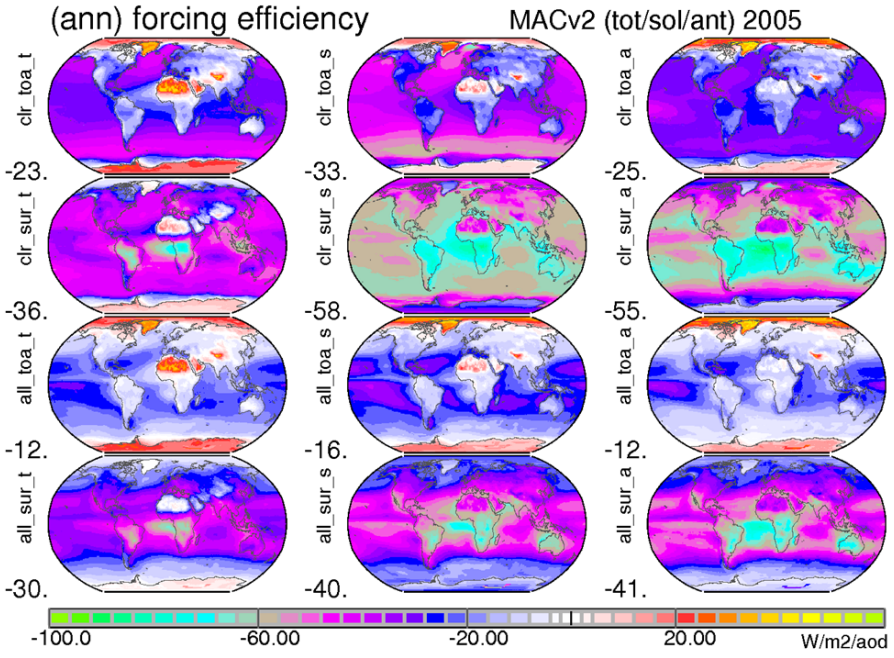

Figure 10 *Annual maps for aerosol direct radiative effect efficiencies (per unit AOD) of present-day all aerosol (left), its solar effect only (center) and of present day anthropogenic aerosol (right). All maps correspond to direct radiative effects presented in Figure 5: Clear-sky efficiencies are presented in the upper rows: at TOA (row 1) and at surface (row2). All-sky efficiencies (with ISCCP clouds) are presented in the lower rows: at TOA (row 3) and at surface (row 4). Values below the label indicate global averages.*

At TOA, on a global average basis, direct aerosol radiative efficiencies (per unit AOD) are at -24 W/m2 for cloud-free conditions (clear-sky) and at -12 W/m2 for realistic conditions with clouds (all-sky). These global averages are almost identical for both total and anthropogenic aerosol. This is a coincidence as for total aerosol a ca 30% stronger solar cooling efficiency is partially offset by a coarse-mode associated IR warming efficiency. Spatially, however, there are large differences associated with aerosol absorption and size and associated with background reflectance (e.g. surface albedo) data.

At the surface global averages for the direct aerosol 'solar only' radiative efficiencies (per unit AOD) for total and anthropogenic aerosol agree at -56 W/m2 cloud-free conditions (clear-sky) at -41 W/m2 for realistic conditions with clouds (all-sky). Average efficiencies for total aerosol are ca 30% less negative with the inclusion of infrared warming (mainly from elevated mineral dust).

Atmos. Chem. Phys. Discuss., https://doi.org/10.5194/acp-2018-949
Manuscript under review for journal Atmos. Chem. Phys.
Discussion started: 3 January 2019

Atmospheric Chemistry and Physics Discussions

With the AOD attributions in MACv2 via their mid-visible absorption properties into radiatively defined aerosol types (*Kinne, 2018*) also TOA efficiencies for aerosol components can be determined and are presented for clear-sky and all-sky conditions in Figure 11.

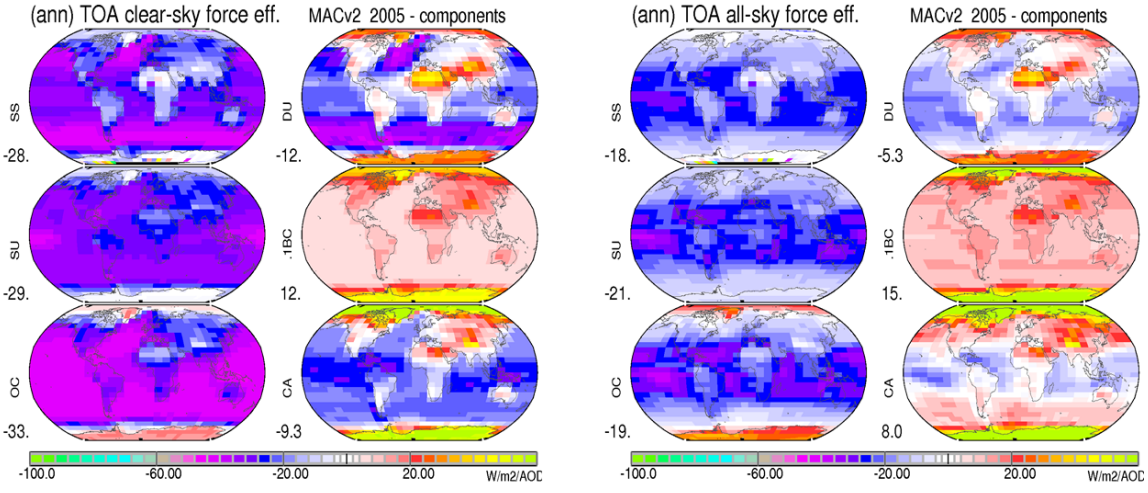

Figure 11 *Annual maps for present-day direct component forcing efficiencies (per unit AOD) at TOA at clear-sky (left block) and at all-sky conditions (right block) by components of sea-salt (SS), non-absorbing fine-mode (SU), organic matter (OC), dust (DU), soot (BC) and for the combined carbon (CA=OC+BC). Note, the larger forcing efficiencies for BC are divided by 10 to fit the common scale. Global averages are presented below the labels.*

Global average component direct radiative TOA efficiencies (per unit AOD) for sulfate, organic matter or sea-salt are near -30 W/m2/AOD for clear-sky conditions and near -20 W/m2/AOD for all-sky conditions. In contrast, direct radiative TOA efficiencies (per unit AOD) for soot (BC) are not only different in sign (positive) but also stronger at +120 W/m2/AOD for clear-sky conditions and at +150 W/m2/AOD for all-sky conditions. Note, the BC efficiency for all-sky conditions is higher because BC dims the solar reflection from lower altitude clouds. In combination with likely co-emitted organic matter (CA =BC+OC), however, the BC efficiencies are strongly reduced to -10W/m2/AOD at clear-sky and to +10W/m2/AOD at all-sky conditions. For dust, positively efficiencies over continents (and especially over the Sahara) and negative efficiencies over oceans largely offset each other for a relatively small global average forcing efficiency. And with that overall small climate impact potential by mineral dust, even larger uncertainties (e.g. on what fraction of present-day dust is anthropogenic) seems less relevant in understanding the aerosol direct forcing.

Atmos. Chem. Phys. Discuss., https://doi.org/10.5194/acp-2018-949
Manuscript under review for journal Atmos. Chem. Phys.
Discussion started: 3 January 2019

7 Aerosol Indirect Effects

Extra atmospheric aerosol loads (as from anthropogenic sources) modulate the atmospheric energy distribution not only by the added aerosol presence (direct effects) but also by changes to environmental properties which in turn modulate the atmospheric energy distribution (indirect effects). An important aspect is that added aerosols (relatively numerous from anthropogenic fine-mode sources) increase the concentrations of those aerosols that can serve as cloud condensation nuclei (CCN). With more available CCN at a condensation event, the available supersaturated water vapor is then distributed around more aerosol particles, so that the resulting water cloud droplets are more numerous and smaller. Assuming no change to the cloud liquid water content (LWC), with smaller drop sizes the solar reflection of a water cloud and along with it the planetary albedo increases (*Twomey, 1974*) for an added climate cooling. Examples are so-called 'ship tracks', when satellite sensors detect increases in planetary albedo of low altitude clouds above the path of polluting ships. But there are further impacts associated with then smaller droplets affecting both cloud cover and cloud water content. For instance, the mixing with dryer air at cloud boundaries reduces the cloud lifetime (especially if cloud cover is low), whereas the delay in the onset of precipitation extends the cloud lifetime (especially if cloud cover is high). Similarly there are also potential but less investigated aerosol impacts involving mixed-phase and ice clouds.

The strongest observational evidences for aerosol indirect effects involve low altitude water clouds. In contrast, aerosol impacts for mixed phase clouds are relatively small (*Christensen et al. 2016*) and aerosol impacts on ice-clouds suffer from much lower aerosol concentrations at higher altitudes and/or the primary need for mineral dust aerosols to serve as (effective) ice-crystal nuclei. Even with the focus on lower altitude water clouds, there remains the question, if changes to cloud lifetime and/or cloud cover matter in comparison to the smaller droplet size (Twomey-) effect. That indeed a smaller droplet effect is the dominant aerosol indirect effect response is demonstrated by a recent satellite retrieval analysis involving a large sulfate aerosol anomaly over the northern Atlantic (*Mallavelle et al., 2017*) with significant reductions to the droplet size yet no significant changes to the liquid water content.

It seems straightforward to convert MACv2 suggested CCN increases due to anthropogenic AOD in cloud droplet number concentration (CDNC) increases (and subsequently in associated cloud droplet size reductions, assuming that the cloud water content did not change). Unfortunately, MACv2 based CCN estimates (derived from fine-mode composition and extinction) depend strongly on assumptions for the supersaturation (or vertical winds at cloud base), which are not known nor can be appropriately represented by averages. To make matters worse, uncertainties affect not only current CCN but also background CCN estimates, as both are needed to derive CDNC changes - due to CCN saturation effects.

Thus, a simpler approach based on satellite retrievals was selected which directly links aerosol number with cloud droplet number, as explained in more detail in Appendix A. It involved retrievals of the fine-mode AOD (AODf) as a proxy for aerosol number and CDNC retrievals at the upper boundary of low altitude clouds as proxy for cloud droplet number. Based on multi-spectral sensor data both properties can be retrieved but not simultaneously at the same time and location. However, there is reliance, that regional associations will provide the needed link. Combining all matches over oceans,

Atmos. Chem. Phys. Discuss., https://doi.org/10.5194/acp-2018-949
Manuscript under review for journal Atmos. Chem. Phys.
Discussion started: 3 January 2019

Atmospheric Chemistry and Physics Discussions

where both, quality CDNC (cloud top) retrievals and sufficient large AODf (the assumed proxy for aerosol number) retrievals, were available, a logarithmic relationship was extracted, which did not significantly change with the use of different satellite sensor data, as demonstrated in Appendix A. The resulting relationship allows to extract CDNC increase factors from an increases in AODf. This meant that CDNC increases depend not only on extra anthropogenic aerosol but also on reference background conditions.

CDNC, factor = ln (1000*AODf [natural +anthropogenic] +3) / ln (1000*AODf [natural] +3)

The satellite derived CDNC factor increase (CDNC, factor) is more moderate than that of an AeroCom global model ensemble, as shown in Appendix A. This demonstrates that Twomey effects (associated with extra anthropogenic aerosol) are on average over-parameterized in most global models.

In an application the CDNC increase factor of the above equation was globally applied at every grid point, thus also over continents where no and not sufficiently accurate satellite retrievals were available. After the CDNC increase factors are converted into cloud droplet radius reductions (assuming no changes to the water content) two scenarios were simulated in an off-line radiative transfer code: One scenario with a reduced cloud droplet size according to local CDNC increases in low altitude clouds and on scenario with the base-line droplet size. The differences of these two simulations define the aerosol indirect effects in MACv2. Present-day annual average indirect effects for the solar and the infrared spectral region at TOA and surface are presented for the MACv2 and (an alternate) MACv1 anthropogenic fractions in Figure 12.

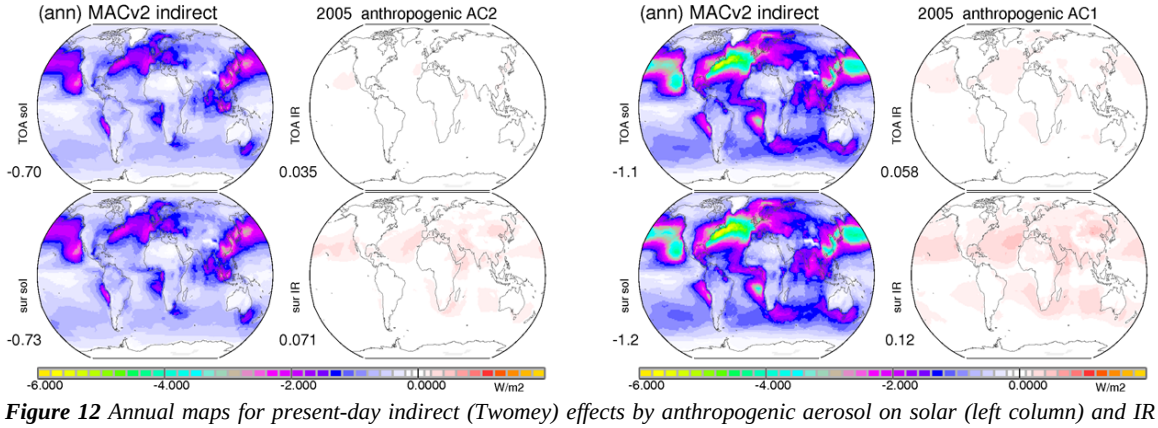

Figure 12 *Annual maps for present-day indirect (Twomey) effects by anthropogenic aerosol on solar (left column) and IR (right column) radiative net-fluxes at the top of the atmosphere (top) and at the surface (bottom). Impacts with (standard) anthropogenic AOD based on AeroCom 2 simulations (left block, AC2) are compared to impacts with anthropogenic AOD based on AeroCom 1 emissions (right block, AC1). Blue colors indicate a 'cooling' and red colors a 'warming'. Values below the labels are global averages.*

Atmos. Chem. Phys. Discuss., https://doi.org/10.5194/acp-2018-949
Manuscript under review for journal Atmos. Chem. Phys.
Discussion started: 3 January 2019

Atmospheric Chemistry and Physics Discussions

The Twomey aerosol indirect radiative effect is mainly a solar response with an increase in the planetary albedo and a complementary decrease to the solar surface net-flux, mainly by a smaller droplet size and also by a slightly increased cloud optical depth (as the cloud water content was not allowed to change). For present-day MACv2 anthropogenic aerosol in the context of the MACv2 pre-industrial (natural) background the global average aerosol solar indirect effects at both TOA and surface are about -0.7 W/m2. There is a lot of spatial variability with the largest contributions over oceans (helped by their dark backgrounds) and over the (by anthropogenic emission mainly affected) Northern Hemisphere. In contrast, to these solar responses, infrared warming is relatively small and at almost negligible +0.04 W/m2 for the TOA indirect forcing. Indirect radiative effects on the atmosphere (e.g. heating) are similarly small, as demonstrated by the differences between TOA and surface effects. Spatial variations on the simulated present-day aerosol indirect effect on a monthly basis are presented in Figure 13.

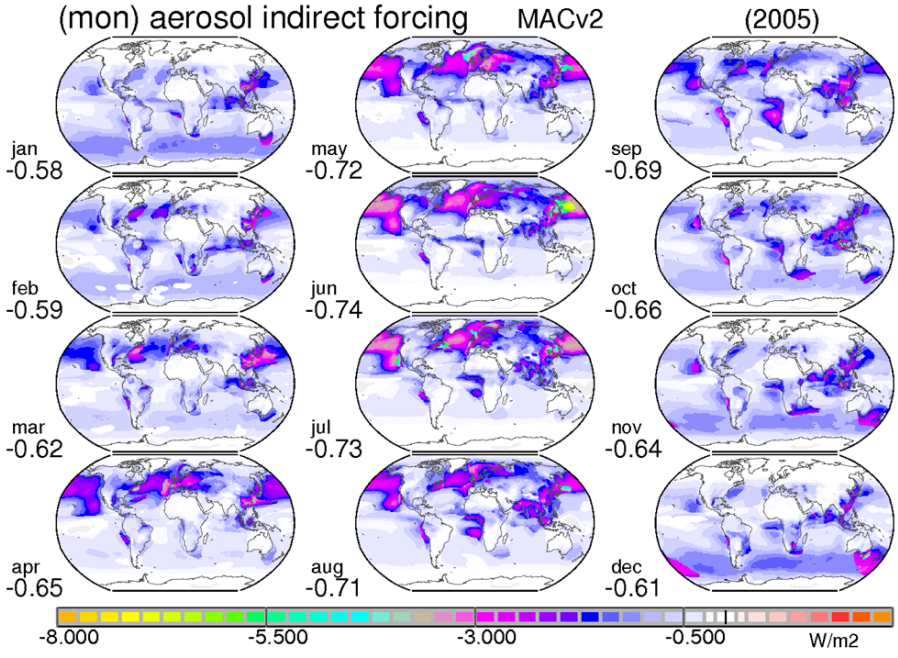

Figure 13 *Monthly maps for today's indirect (Twomey) forcing by present-day anthropogenic aerosol*

The present-day aerosol indirect forcing is not just influenced by anthropogenic aerosol and/or background aerosol conditions but also by environmental properties. The indirect forcing is strongest over the mid-latitude oceans (with relative

dark surface), during spring and summer (with longer sun-shine hours) and mainly the Northern Hemisphere (where most anthropogenic aerosol is found). In comparison, indirect effects over stratocumulus regions are rather moderate.

Figure 12 also presents results with a higher anthropogenic fine-mode fraction, as they were used in MACv1 (*Kinne et al, 2013*) based on AeroCom emission data (*Dentener et al., 2006*). With the alternate 30% larger anthropogenic AOD the aerosol indirect forcing increase is at 50% even stronger, yielding a present-day indirect aerosol forcing of -1.1W/m2. The stronger than expected response is explained by a smaller natural background (as a consequence of the increased anthropogenic fraction) so that the CDNC change potential through the logarithmic relationship is increased. Thus, the indirect aerosol forcing is very sensitive to anthropogenic assumptions and more sensitive than for the direct forcing (which at the climate impact relevant TOA is also on average smaller).

The aerosol indirect forcing, however, does not only depend on the anthropogenic aerosol and natural aerosol background, but also on environmental properties, such as solar energy, sun elevation, solar surface albedo, single layer low altitude cloud and a moderate cloud optical depth for highest susceptibility. Extra analysis of indirect forcing potential and indirect forcing efficiency is provided in Appendix F. Due to very low aerosol natural background conditions, indirect forcing efficiencies over Southern Oceans can be very high. Although indirect effect contributions from those regions are only minor, possible indirect effect overestimates in these regions cannot be ruled out, even more so as the applied section of the AODf vc CDNC relationship is not observationally constrained at very low AODf.

8 Direct vs Indirect

MACv2 associated aerosol present-day direct and indirect radiative effects are now compared. Annual maps for TOA direct radiative effects with clouds (forcing) and without clouds, for TOA indirect forcing and for the combined (direct and indirect) forcing are presented in Figure 14.

Atmos. Chem. Phys. Discuss., https://doi.org/10.5194/acp-2018-949
Manuscript under review for journal Atmos. Chem. Phys.
Discussion started: 3 January 2019

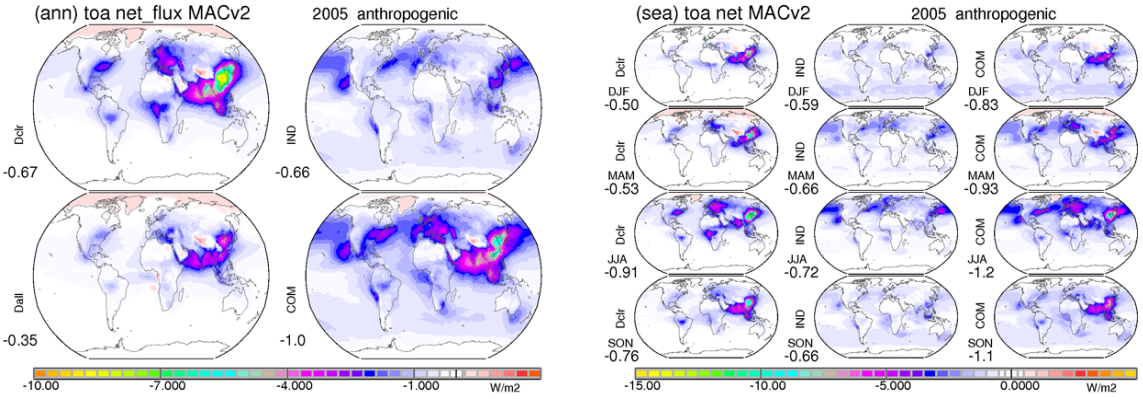

Figure 14 *TOA radiative effects by present-day anthropogenic aerosol. Annual (left block) and seasonal maps (right block) compare direct radiative effects at clear-sky conditions (Dclr) and all-sky conditions (Dall), aerosol indirect (Twomey) effects through modified clouds (IND) and the combined (direct and indirect) effect (COM). Blue colors indicate 'cooling' net-flux losses and (rare) red colors indicate 'warming' net-flux gains. Values below the labels indicate global averages.*

At the TOA climate cooling by the present-day indirect effect (globally averaged at -0.66 W/m2) is about twice as large as the present-day direct effect (globally averaged at -0.35 W/m2). However, the spatial variability of the local direct forcing is much more diverse, as there are even regions with local climate warming (through dimming over snow, over lower cloud or during polar nights). The combined climate impact is a cooling (globally averaged at -1.0 W/m2) with cooling everywhere except over Greenland. The present-day clear-sky cooling is about 60% of the combined (direct and indirect) cooling. Thus, (the presence of) clouds contribute with 40% to (present-day) aerosol climate cooling. Since anthropogenic AOD values are higher over the northern hemisphere, the climate cooling by aerosol in those region is larger. Hereby the direct effect dominates near continental sources while the indirect effect has stronger impacts over oceanic regions away from sources. With larger AOD, less snow cover and more sunshine both indirect and direct present day forcing display maximum impacts during the northern hemispheric summer season. Monthly maps for the present-day combined direct and indirect forcing are shown in Figure 15 and those for all TOA contributions at common scale are presented in Appendix C.

Atmos. Chem. Phys. Discuss., https://doi.org/10.5194/acp-2018-949
Manuscript under review for journal Atmos. Chem. Phys.
Discussion started: 3 January 2019

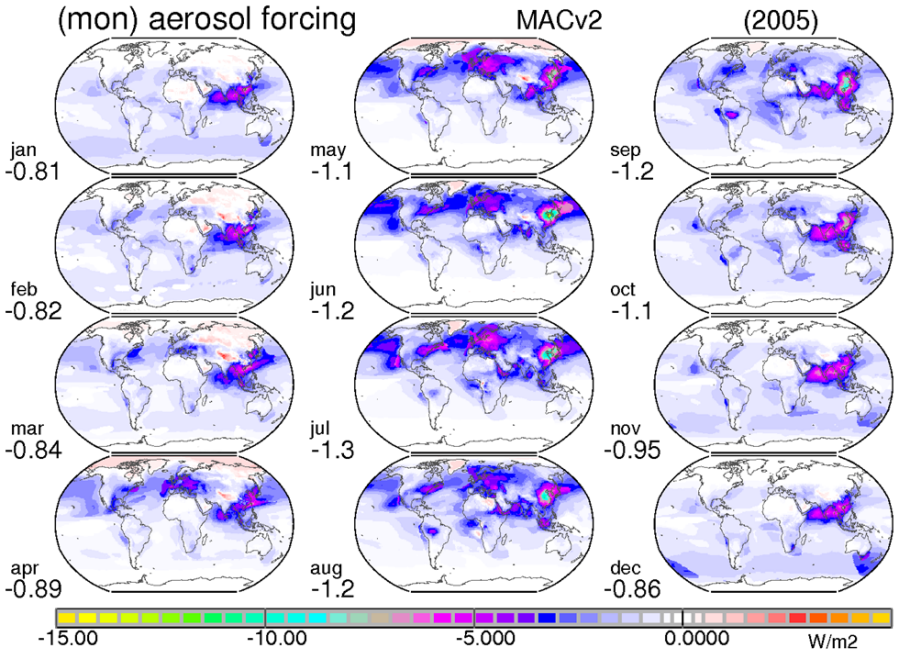

Figure 15 *Monthly maps for today's total forcing by present-day anthropogenic aerosol*

Present-day radiative effects at the surface and for the atmosphere are compared in Figure 16. With the radiative solar absorption and atmospheric heating by the present-day direct effect by about +1.1 W/m2, radiative losses at the surface of the direct effect are now that much larger at -1.45 W/m2. Since indirect effect net-flux losses at the surface closely resemble those at TOA (both at -0.66W/m2) now (in contrast to the indirect effect dominance at TOA) the total radiative losses of -2.1 W/m2 by present-day anthropogenic aerosol is pre-dominantly contributed via the direct effect.

Atmos. Chem. Phys. Discuss., https://doi.org/10.5194/acp-2018-949
Manuscript under review for journal Atmos. Chem. Phys.
Discussion started: 3 January 2019

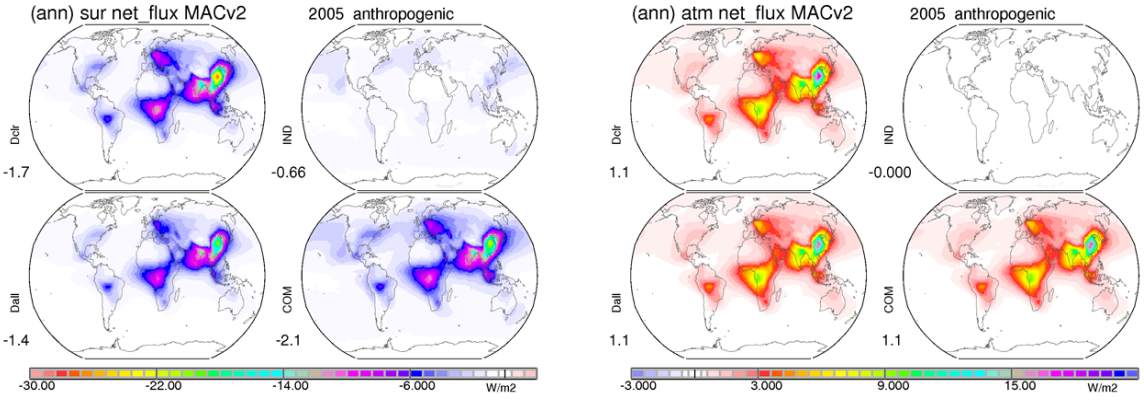

Figure 16 *Annual radiative effects by present-day anthropogenic aerosol at the surface (left block) and for the atmosphere (right block). Maps compare direct effects at clear-sky conditions (Dclr) and all-sky conditions (Dall), indirect (Twomey) effects through modified clouds (IND) and the combined (direct and indirect) effect (COM). Blue colors indicate 'cooling' net-flux losses and red colors indicate 'warming' net-flux gains. Values below the labels indicate global averages.*

Interestingly the clear-sky direct impact (1) on a global average basis and (2) in captioning the major regional impact maxima (upper left of the left block in Figure 16) is quite similar to the combined (direct and indirect) impact (lower right of the left block in Figure 16). Certainly there are smaller differences, especially in remote regions, but for rough estimates on the aerosol impacts, already clear-sky radiative simulations could provide useful climate impact estimates.

9 Forcing over Time

The MACv2 aerosol climatology offers global maps for anthropogenic AOD over time (as illustrated in Figure 3). Results of radiative transfer simulations that apply these changing anthropogenic AOD data with time are presented in Figure 17. There annual maps for direct effects at cloud-free conditions, for the cloud presence influence on the cloud-free effect (a relative warming), for the indirect (Twomey) forcing (a cooling) and for the summarizing total forcing are presented.

The cloud-free direct effect cools the climate. The clouds modulate this clear-sky cooling with a (relative) warming by the cloud presence and with an extra cooling via the indirect effect. Overall the cloud's influence is a cooling. And total cooling is even stronger than the direct cooling. The forcing components over time show, in agreement with the logarithmic relationship, that ratio between indirect versus direct forcing contributions was higher at lower aerosol background concentrations as in the early years of the industrial revolution than it is presently.

The temporal time-slice maps demonstrate that early into the industrial period mainly the US and Europe where affected by aerosol cooling. By 1985 with SE Asia a third affected region had emerged. Since then the aerosol cooling over

Atmos. Chem. Phys. Discuss., https://doi.org/10.5194/acp-2018-949
Manuscript under review for journal Atmos. Chem. Phys.
Discussion started: 3 January 2019

Atmospheric Chemistry and Physics Discussions

SE Asia kept on growing while climate cooling by aerosol over Europe and the US declined, also due to successful mitigations efforts. With these opposing regional shifts during the last decades the global average aerosol cooling stayed just below -1.0 W/m2. As in the meantime (ca by 2015) anthropogenic aerosol loads had reached their regional maximum over E Asia (while not yet over S Asia) no further increases for future aerosol cooling are being expected, even if some future emission projections indicate the development of a new maximum over W. Africa.

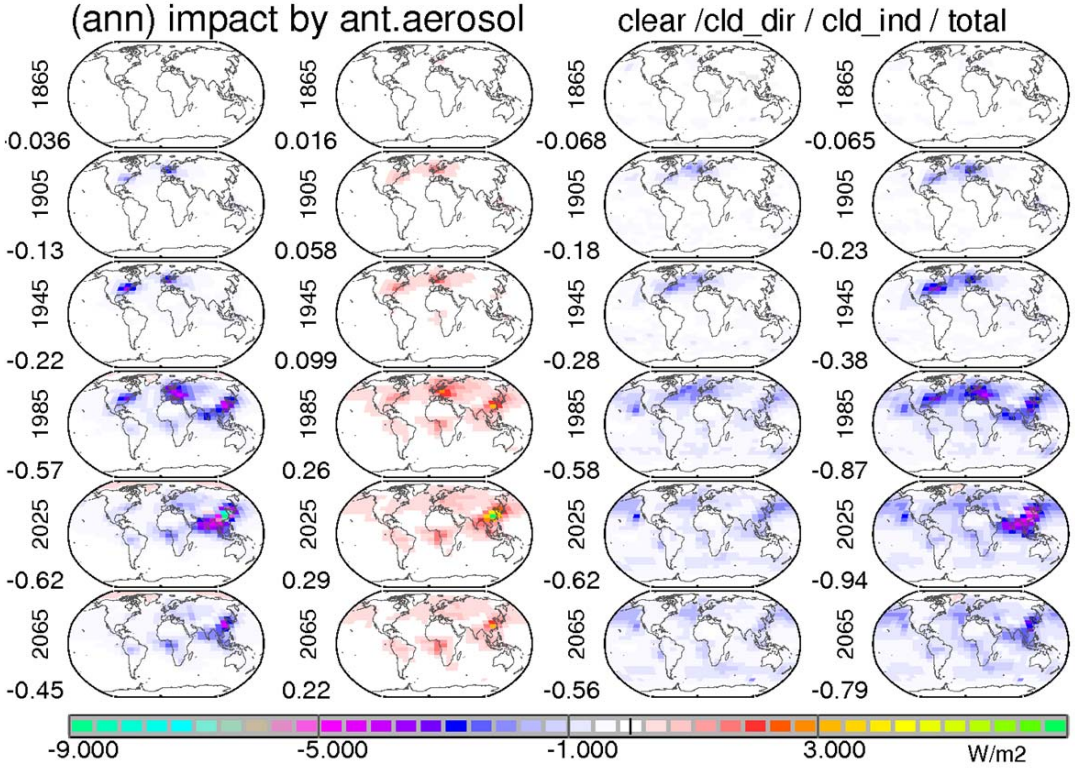

Figure 17*. Comparing annual average impacts by anthropogenic aerosol on TOA radiative fluxes as a function of time (for selected years of 1905, 1945, 1985, 2025 and 2065) for the total radiative forcing (column 4) and contribution components: clear-sky radiative effect (column 1), the cloud presence effect on the clear-sky radiative effect (column 2) and the indirect (Twomey) forcing (column 3). Values below the labels indicate global averages.*

A different way to illustrate changes and regional shifts associated with extra anthropogenic aerosols are difference over selected time-periods as illustrated in Figure 18. In that figure changes for the aerosol radiative effects over four 40 year

time-intervals *(1865-1905, 1905-1945, 1945-1985, 1985-2025)* are compared. Hereby aerosol changes to (1) clear-sky effects, (2) all-sky effects and (3) combined (direct and indirect) effects to TOA and surface net-fluxes are shown.

Climate cooling by aerosol strongly increased over Europe and SE Asia between 1945 and 1985. Between 1985 and 2025 aerosol cooling continued to increase over SE Asia, whereas aerosol cooling decreased over Europe and Northern America during the period. Hereby changes to the surface fluxes (with a stronger direct signature) are much larger than changes to fluxes at the TOA. These regional changes over the last decade are consistent with observations by ground-based radiation (*Wild, 2015*), which in particular for Europe diagnosed a dimming (until 1985) following by a brightening (since 1985).

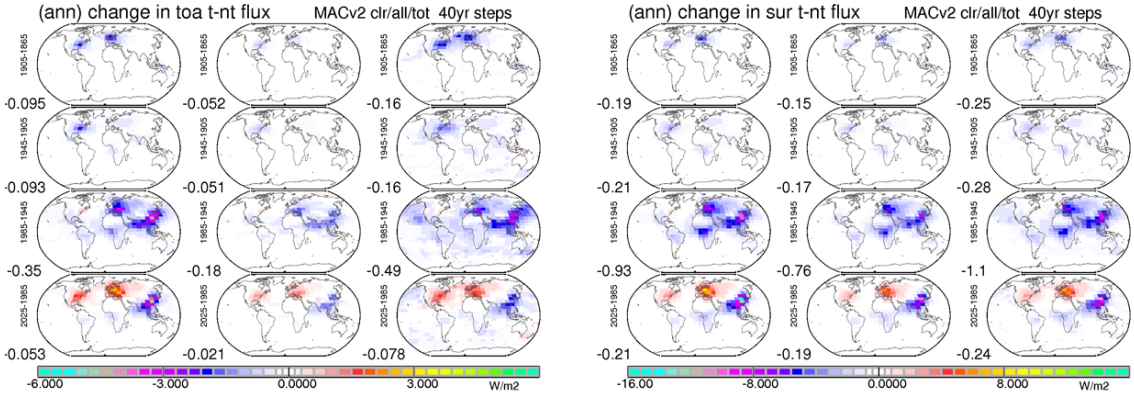

Figure 18*. Changes in aerosol radiative effects at TOA (left block) and at the surface (right block) for four 40 year time periods (1865-1905, 1905-1945, 1945-1985, 1985-2025) for direct clear-sky (left column), direct all-sky (center column) and combined direct and indirect effects. Blue colors indicate increased cooling by aerosol, while red colors indicate a reduced cooling by aerosol. Note the different scales, as radiative effects at the surface are larger. Values below the labels indicate global average differences.*

10 Uncertainty

The calculation of the aerosol radiative effects and the aerosol radiative forcing include many uncertainties. The focus here is on uncertainties to the aerosol fields of the MACv2 (although also radiative transfer model, environmental data and the use of monthly average contribute). An initial test in Figure 19 compares the impact of a different background in developing the aerosol climatology.

Atmos. Chem. Phys. Discuss., https://doi.org/10.5194/acp-2018-949
Manuscript under review for journal Atmos. Chem. Phys.
Discussion started: 3 January 2019

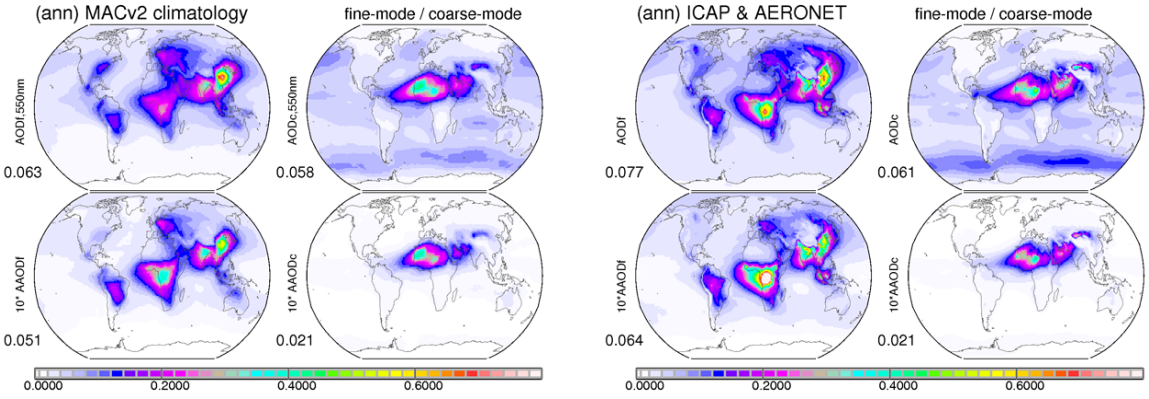

Figure 19 *estimates of today's annual maps for tropospheric AODf, AODc, AAODf and AAODc by combining AERONET data with an AeroCom1 median (left block) and with satellite AOD data assimilating ICAP averages (right block). AAOD data are multiplied by 10. Values below labels show global averages.*

As alternate background ICAP ensemble data (*Peng et al., 2018*) from the satellite AOD assimilation community are used and impacts on fine-mode and coarse-mode AAOD data are presented.

The climatology with the ICAP background yields on average ca 15% larger values for the mid-visible AOD. Patterns are slightly shifted but major differences are much stronger fine-mode AOD and AAOD maxima over central Africa. If this difference is the result of satellite AOD retrieval overestimates or due to overlooked emissions in modeling is difficult to judge, as no AERONET reference sites in that region are available. Globally the fine-mode AOD, which also defines via a model extracted fraction the anthropogenic AOD, is ca 25% larger. Fortunately, most of this extra fine-mode AOD has a strong natural component so that the anthropogenic AOD is increased by just 10% as shown in Figure 20.

Atmos. Chem. Phys. Discuss., https://doi.org/10.5194/acp-2018-949
Manuscript under review for journal Atmos. Chem. Phys.
Discussion started: 3 January 2019

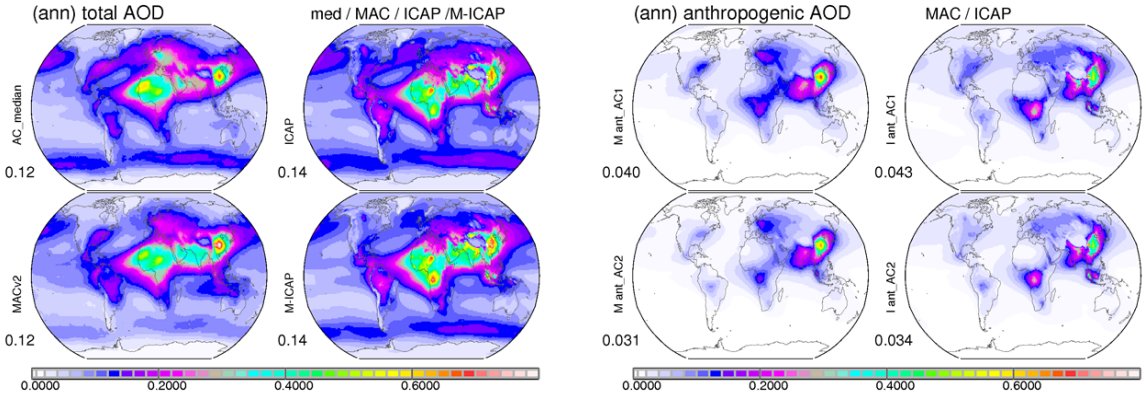

Figure 20 *uncertainty estimates for present-day total and anthropogenic AOD from different realizations. Annual maps for tropospheric total AOD (left block) and for anthropogenic AOD (right block) are shown. Total AOD maps compare model-ensemble data of AeroCom1 experiments (left column) and ICAP satellite data assimilations (right column), before (top) and after (bottom) the data merging with sun-photometer data. Anthropogenic AOD maps are results of applying the two different anthropogenic fractions (based on emissions by Dentener - AC1 and Lamarque - AC2) to the fine-mode AOD of the AERONET adjusted maps. Values below the label show global averages.*

The assumed anthropogenic fraction for present-day aerosol introduces another and (probably the main) uncertainty. Potential coarse mode anthropogenic contributions via mineral dust (e.g. due to land use change) seem secondary, because dust forcing is near neutral. For the fine-mode AOD (AODf) anthropogenic contributions are defined via a fine-mode anthropogenic fraction from modeling applied the AODf of MACv2. Aside from the standard anthropogenic fine-mode fraction in MACv2 based on model simulations with IPCC5 emissions (*Lamarque et al., 2010*) in addition an alternate anthropogenic fine-mode fraction based on AeroCom emissions (*Dentener et al., 2006*) is applied. With the alternate larger anthropogenic fraction the MACv2 anthropogenic AOD increases from 0.031 to 0.040, as shown in Figure 20 - an increase by 30%. And if the alternate ICAP background was used in place of the AeroCom background then there is another increase of ca 10% to 0.034 and 0.043, respectively. Even considering that the alternate anthropogenic fine-mode fraction based on AeroCom emissions is based on a year 1750, which does not really applies for a year 1850 reference, still a 0.030 to 0.038 range for the present-day the anthropogenic mid-visible AOD should be allowed, thus a 25% uncertainty.

Sensitivity studies in Appendix B demonstrate that a 25% larger anthropogenic AOD means a 25% stronger direct forcing and a 40% larger indirect forcing. In addition with a different merging of sun-photometer data in MACv2 (with ICAP modeling) a 15% larger total AOD, causing similar increases to the aerosol direct and aerosol indirect forcing cannot be ruled out. Thus, a 0.7 to -1.6 W/m2 range is estimated for present-day aerosol forcing (since year 1850), with the best guess value at -1.0 W/m2.

The main argument for the upper bound -1.6 W/m2 in climate cooling is that the anthropogenic AOD fraction in theory can be larger. It is shown (in Appendix B) that with the larger anthropogenic fine-mode fraction of MACv1, with the

MACv2 aerosol properties the aerosol indirect effect increases (from -0.65) to -1.1 W/m2 and the direct effect (from -0.35) to -0.5 W/m2. The applied MACv1 anthropogenic fraction (based on year 1750 emissions) however, is likely overestimated with respect to year 1850 but a 25% larger anthropogenic AOD should still be considered. However, a potentially lower upper bound evaporates by the possibility of a ca 15% larger AOD, as demonstrated with the use of the alternate ICAP ensemble background of Figure 19.

The main argument for the lower bound of -0.7W/m2 in climate cooling is a lower bound of the (better constrained) direct effect at -0.2W/m2 via the possibility of a larger BC anthropogenic fraction and a -0.5W/m2 minimum cooling via the (Twomey) indirect effect.

To reduce the aerosol forcing range (-0.7 to -1.6 W/m2) progress in quantifying the indirect effect(s) and pre-industrial references for all aerosol components are needed.

11 Summary

The MACv2 global monthly aerosol climatology, tied to observational monthly statistics on aerosol amount, absorption and size from sun-/sky-photometry, was applied in dual-call off-line radiative transfer to determine aerosol effects on atmospheric radiation. The direct (added presence) effects of present-day aerosol and the climate change relevant effects of anthropogenic contributions (since pre-industrial times) are determined. Hereby results are usually presented via global annual and even monthly maps to visualize regional and temporal detail, as not only aerosol properties but also influential environmental properties have strong regional and seasonal signatures. Still, for simplicity, most discussions below apply resulting global annual averages. Hereby radiative netflux changes are examined at the climate relevant TOA location, at the surface for exchange processes near the ground and for the atmospheric dynamics (via the TOA minus surface impact). Radiative netflux losses refer to a cooling and radiative netflux gains refer to a warming.

Present-day total aerosol by its presence (direct effect) reduces netfluxes by -1.1 W/m2 at the TOA and by -4.0 W/m2 at the surface, so that the energy in the atmosphere is increased by +2.9 W/m2. Hereby, the netflux losses are composed of larger solar losses and a partly offsetting smaller infrared gains, at -1.8 and +0.7 W/m2 at the TOA and -5.5 and +1.5 W/m2 at the surface, while atmospheric solar warming of +3.7 W/m2 is reduced by -0.8 W/m2 in atmospheric IR cooling.

Anthropogenic aerosol is only considered to contribute to sub-micrometer aerosol sizes so that only solar radiative effects matter (IR radiative effects can be neglected). Present-day anthropogenic aerosol by its added presence (direct effect) reduces netfluxes by -0.36 W/m2 at the TOA and by -1.5 W/m2 at the surface, so that the energy in the atmosphere is warmed by +1.1 W/m2. In addition, also impacts via low altitude cloud changing microphysical properties (indirect effect) are considered via a satellite retrieval association derived relationship between aerosol and cloud-drop concentrations. The indirect effect reduces mainly solar radiative netfluxes at the TOA and at the surface by -0.65 W/m2. Thus the combined direct and indirect yields a cooling of -1.0 W/m2 at the TOA and of -2.1 W/m2 at the surface. Hereby the climate cooling at

the TOA is dominated by the indirect effect, while the cooling at the surface is dominated by the direct effect. And the direct effect is solely responsible for the atmospheric heating. Spatially both direct and indirect effects are strongest during the NH summer. Direct effects are strongest near continental sources. Indirect effects are stronger away from sources over (dark) oceans.

Uncertainties with respect to the aerosol properties should consider that the total AOD could be 15% larger and that a 25% larger anthropogenic fraction is possible. Simulations with a 30% larger anthropogenic fraction, as used in MACv1 (*Kinne et al, 2013*) yield a 30% larger direct effect and an even 50% larger indirect effect. Thus, the uncertainty for present day forcing (the anthropogenic impact at the TOA) is between -0.7 and -1.6 W/m2, with -1.0 W/m2 as the best estimate. Hereby, the direct effect is much better constrained (-0.20 to -0.45 W/m2) than the indirect effect (-0.5 to -1.1 W/m2). A better estimate for the pre-industrial reference would help in reducing these uncertainties. And also the rather simple representation of the indirect effect should be validated.

As MACv2 optical properties also allow to attribute component contribution estimates for the (aerosol presence) direct effect of components are offered. These 'top-down' component present-day forcing values agree with those from 'bottom-up' modeling, as summarized in Appendix G. Present-day total soot (BC) warms at the TOA with +55 W/m2, where at least half of that warming can be attributed to anthropogenic sources. With the possibility of an anthropogenic fraction for soot (BC) that is larger than for the fine-mode fraction (in other words that the anthropogenic aerosol is more absorbing than the natural background fine-mode aerosol) present warming by anthropogenic BC could be raised (from now +0.28 up to +0.38 W/m2) which in turn would reduce the present-day direct forcing to a -0.25W/m2 cooling and total forcing to a -0.9W/m2 cooling. Thus, not only accurate information on the pre-industrial state of the fine-mode AOD but also on its components at that time (e.g. soot properties) is needed.

The combined carbon (BC and OC) component, which approximates effect of BC co-emitters has (without a higher BC anthropogenic fraction) a near neutral forcing behavior. Thus, short term climate warming mitigation concept via a soot removal may not be too effective as also scattering aerosol resulting from co-emitted trace-gases would be removed. The climate impact for mineral dust (while showing strong warming over continents, yet strong cooling over oceans) behaves globally almost climate neutral. Thus, potential anthropogenic impacts from dust, as a result of land-use change, as uncertain as they are, seem less importance for climate change considerations. Thus in the end it are the (in the mid-visible) non-absorbing sub-micrometer size aerosol (mainly sulfate and nitrate) that regulate the anthropogenic AOD.

Calculations with model predicted temporal changes to the anthropogenic AOD indicate that qualitatively the anthropogenic aerosol forcing has not changed much over the last decades and is not likely to increase over the next decades, despite strong regional shifts. These regional shifts explain most solar insolation (brightening or dimming) trends that have been locally observed by decadal time-series ground-based radiation, especially over Europe and the US.

Resources

MACv2 properties are accessible at ftp://ftp-projects.zmaw.de/aerocom/climatology/MACv2_2018/ .
The data are placed in several subdirectories and a README file describes data content of file-names

- /550nm (mid-visible) aerosol properties at 550nm wavelength
- /CCN lower cloud-base condensation nuclei and critical radii at diff. supersaturation
- /detail ancillary data for radiative transfer simulations
- /documents some documentation and figures
- /forcing MACv2 associated radiative effects
- /retrieval MACv2 fields for under-determined solar reflection based AOD retrievals
- /spectral 2005 optical data at 3 different spectral resolutions: 20, 30 (RRTM),31 bands
- /time same as in /spectral … but data for different years (from 1850 to 2100)

Acknowledgements

This study relied on observational data when possible. Central to the effort are data provided by the ground-based sunphotometer network of AERONET lead by B. Holben and the MAN network lead by A. Smirnov. Also satellite data of the MODIS and AATSR sensors were applied to quantify aerosol indirect effects. Hereby in particukar CDNC retrievals contributed by D.Grosvenor, J.Rausch and M. Christensen and analysis work by J.Müsse, who created all figures in Appendix A are acknowledged. Another essential element to this study is global model output from simulations with bottom-up processing in aerosol modules as part of the AeroCom initiative lead by M. Schulz and M. Chin. An ensemble median provides data on spatial context, estimates on aerosol anthropogenic fractions (also as a function of time) and aerosol vertical distribution. Thus, all modeling groups contributing to AeroCom experiments are acknowledged. Finally this work was support by EU-projects, in particular the FP7 EU-Bacchus project (603445) lead by U.Lohmann and by ESA's climate initiative, in particular the aerosol-CCI effort lead by T. Popp and G. de Leeuw and coordinated by S. Pinnock.

References

Bellouin, N., Quaas J., Morcrette, J.-J. and Boucher O.: Estimates of the radiative forcing from the MACC re-analysis, Atmos, Chem. Phys. 13, 2045-2062, 2013

Bond, T., Doherty S., Fahey D., Forster P., et al.: Bounding the role of black carbon in the climate system: A scientific assessment, Journal of Geophysical Research: Atmospheres Volume 118, Issue 11, 2013.

Christensen, M, Suzuki, K., Zambri, B. and Stephens, G.: Ship track observations of a reduced shortwave aerosol indirect effect in mixed-phase clouds Geopys.Res.Lett. 41, 6970-6977, 2016.

Coakley, J. and Walsh C.: Limits to the Aerosol Indirect Radiative Effect Derived from Observations of Ship Tracks J.Atmos.Sci. 58 668-680, 2002.

Dentener, F., S. Kinne, et al.: Emissions of primary aerosol and precursor gases in the years 2000 and 1750, prescribed datasets for AeroCom, ACP, 6, 4321-4344, 2006.

Dubovik, O., Holben, B., Eck T., Smirnov, A., Kaufman Y., King, M., Tanre, D., and Slutsker, I.: Variability of Absorption and Optical Properties of Key Aerosol Types Observed in Worldwide Locations, J.Atmos.Sci, Vol 38, 580-608, 2002.

Fiedler, S., Kinne, S., Huang, W., Risonen, P., O'Donnel, D., Bellouin, N., Stier, P., Merikanto, J., Carslaw. K., Makkonen J., and Lohmann, U.: Inter-comparison study with your offline estimates of anthropogenic aerosol forcing - insight from multi-estimates from aerosol-climate models with reduced complexity, Atmos. Chem. Phys. Discuss., https://doi.org/10.5194/acp-2018-639, 2018

Fiedler, S., Stevens, B. and Mauritzen, T. : On the sensitivity of anthropogenic aerosol forcing to model-internal variability and parameterizing a Twomey effect, Journal of Advances in Modeling Earth Systems, J. Adv. Mod. Earth Syst., 9, doi:10.1002/2017MS000932, 2017.

Holben, B., Tanre, D., Smirnov, A., Eck, T., Slutsker, I. et al.,: An emerging ground-based aerosol climatology: Aerosol Optical Depth from AERONET, J. Geophys. Res., 106, 12067-12097, 2001

Kinne, S.: The MACv2 Aerosol Climatology, submitted to Tellus B, 2018

Kinne, S., O'Donnel, D., Stier, P., Kloster, S., Zhang, K., Schmidt, H., Rast, S, Giorgetta, M., Eck, T., and Stevens, B.: MAC-v1: A new global aerosol climatology for climate studies, J. Adv. Model. Earth Syst., 5, 704–740, doi:10.1002/james.20035, 2013.

Kinne S., Schulz, M., Textor, C., Guibert, S. et al.: An AeroCom initial assessment – optical properties in aerosol component modules of global models, ACP, 6, 1-22, 2006

Lamarque, J.-F., et al.: Historical (1850-2000) gridded anthropogenic and biomass burning emissions of reactive gases and aerosols: methodology and application, Atmos. Chem. Phys., 10, 7017-7039, doi:10.5194/acp-10-7017-2010, 2010.

McClatchey, R., Fenn, R., Selby. J., Volz, F. and Garing, J.: Optical properties of the atmosphere, Environ. Res. Paper, 411, AFCRL-72-0497, p108, 1972.

Mallavelle, F., Hayward, J. et al.: Strong constraints on aerosol–cloud interactions from volcanic eruptions Nature volume 546, pages 485–491 (22 June 2017) doi:10.1038/nature22974, 2017.

Meador, W. and Weaver, W: Two-stream approximation to radiative transfer in planetary atmospheres: a unified description of existing methods and new improvement, J. Atm. Sci. 37, 630 – 643, 1980

Myhre, G., Samset, B., Schulz, M. et al.: Radiative forcing of the direct aerosol effect from AeroCom Phase II simulations, Atmos. Chem. Phys., 13, 1853– 1877 doi:10.5194/acp-13-1853-2013, 2016.

Peng,Y. et al.: Current state of the global operational aerosol multi-model ensemble: an update from the International Cooperative for Aerosol Prediction (ICAP) QJRMS submitted, 2018

Rossow, W., Walker A. and Garder, C.: Comparison of ISCCP and other cloud amounts, J.Climate, 6, 2394-2418, 1993.

Schaaf, C., F. Gao, F., Strahler, A., Lucht, W. et al.: First oberservational BRDF, albedo and nadir reflectance from MODIS, Remote Sens. Environ., 83, 135-148, 2002.

Schulz M., Textor, C., Kinne, S. et al.: Radiative forcing by aerosols as derived from the AeroCom present-day and pre-industrial simulations Atmos. Chem. Phys., 6, 5225-5246, 2006 doi.org/10.5194/acp-6-5225-2006, 2006.

Stevens, B., Fiedler, S, Kinne, S., Peters, K., Rast, S., Müsse, J., Smith, S., and Mauritsen, T. : MACv2-SP: a parameterization of anthropogenic aerosol optical properties and an associated Twomey effect for use in CMIP6. Geoscientific Model Development, 10, 433-452, 2017.

Smirnov, A., Holben, B., Slutsker, I., Giles, D., et al.: Maritime Aerosol Network as a component of Aerosol Robotic Network, J. Geophys. Res., 114, D06204, doi:10.1029/2008JD011257, 2009.

Taylor, J., Edwards, J., Glew, M., Hignett, P., and Slingo, A.: Studies with a flexible new radiation code. II: Comparisons with aircraft shortwave observations, Q. J. R. Metreorol. Soc., 122, 839– 861, 1996.

Twomey, S.: Pollution and the planetary albedo, Atmos.Environ. 8, 1251-1256, 1974.

Wild, M.: Decadal changes in radiative fluxes at land and ocean surfaces and their relevance for global warming WIREs Clim Change 2016, 7:91 107. doi: 10.1002/wcc.372 , 2015.

Appendix A *the satellite based AODf vs CDNC relationship*

Observational relationships, which employ regional associations between satellite retrieved properties for fine-mode AOD (AODf) and cloud droplet number concentration (CDNC) allow to associate increases in AODf from anthropogenic sources with increases in CDNC. For selected AODf ranges the median CDNC value is determined and then all median CDNC values are combined to result in logarithmic curve fit. By applying the curve twice locally, once for the present-day AODf and once for the pre-industrial AODf an associated CDNC increase in determined. Hereby the CDNC increase depends on the AODf difference and on the AODf (pre-industrial) background. Further assuming that the cloud water of the affected cloud remains constant, CDNC increases are easily converted into drop size reductions, the needed input to simulate associated increases to the planetary albedo, the Twomey effect (*Twomey, 1974*), in off-line radiative transfer simulations.

AODf and CDNC cannot be retrieved by the same sensor at the same time. However spatial associations within larger regions are expected to offer insights on potential relationships. Retrieval averages are matched for relatively large 1x1 degree in latitude/longitude regions. This is in part done to avoid exaggerations in associations, as local indirect effects (e.g. ship pollution impacts) are usually weaker in the context of larger spatial scales (*Coakley and Walsh, 2002*). For better statistics also only monthly averages are matches. Their use seems justified, because at these large spatial scales monthly associations are almost identical to those using daily data instead (*Christensen, private communication*).

Associations between AODf and CDNC were only considered over oceanic regions (where satellite retrievals for both properties are more reliable due to the dark background) and only when both sufficient signal and quality could be

assured. Thus, only CDNC retrievals for overcast conditions under near nadir views are considered. The investigated matches include two different MODIS sensor based CDNC retrievals for an entire year (*collection 5.1, for year 2007 provided by Dan Grosvenor, Leeds and collection 6.0 for year 2008 provided by John Rausch, Vanderbilt*) with matching AODf data from NASA's LAADS site and an ATSR sensor based CDNC retrieval (*for year 2008 provided by Matt Christensen*) for a single season with matching AODf data by RAL's ORAC retrieval. 1x1 degree regions with valid matches between AODf and CDNC data are illustrated in Figure A1.

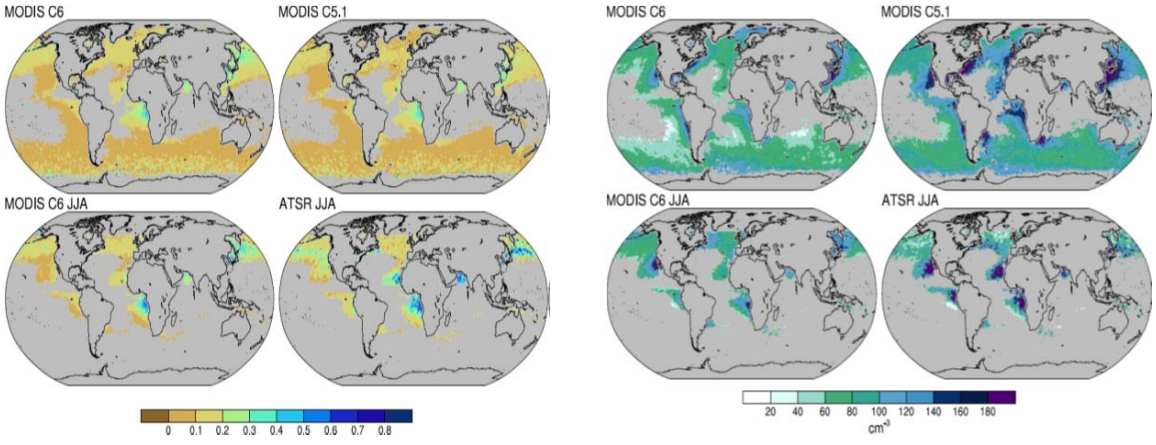

Figure A1 *Annual maps (top) and a JJA seasonal maps (bottom) for AODf (left block) and CDNC (right block) for different retrievals with MODIS and ATSR sensor data.*

Between the three different retrievals for CDNC and AODf there are often larger absolute differences. The more important relative differences (as expressed by the logarithmic shapes, constructed from connection median CDNC points in AODf sub-bins), however, are smaller. The resulting logarithmic fits along with the data scatter are presented in Figure A2. In that figure the AODf to CDNC associations of all available months and locations are combined in a single plot.

Atmos. Chem. Phys. Discuss., https://doi.org/10.5194/acp-2018-949
Manuscript under review for journal Atmos. Chem. Phys.
Discussion started: 3 January 2019

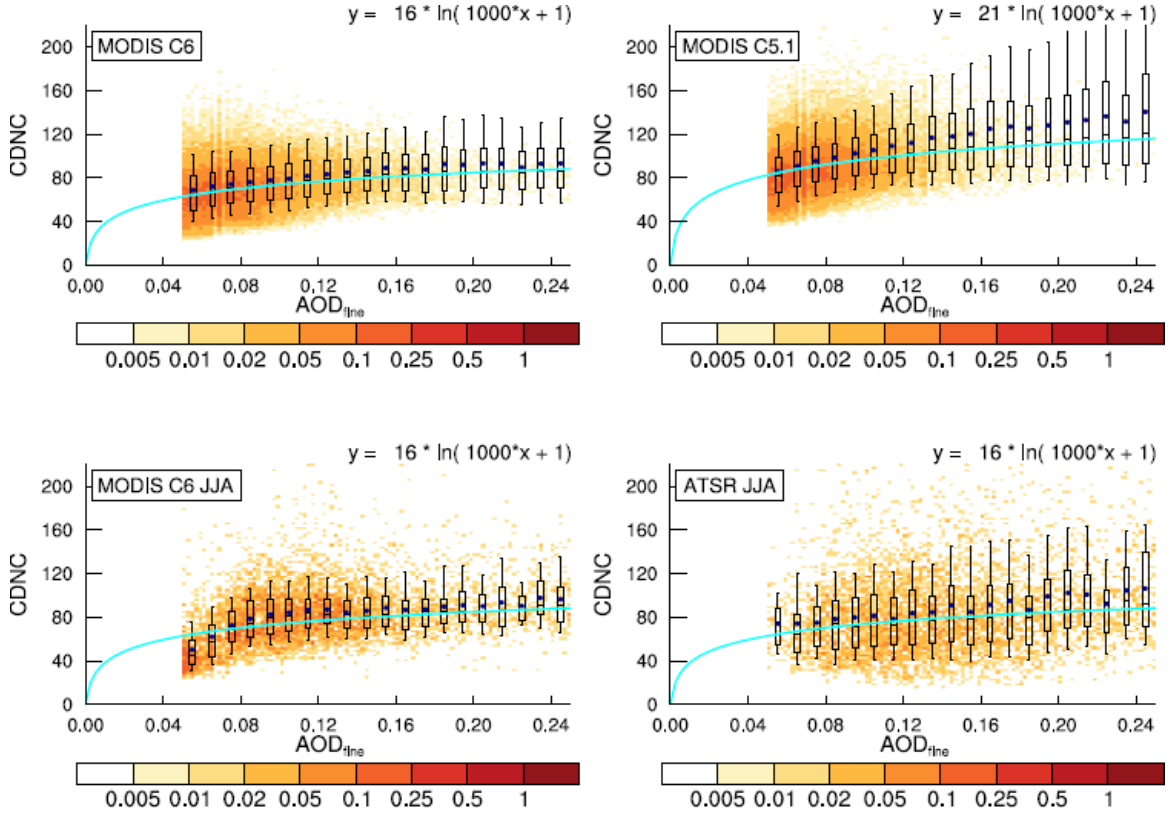

Figure A2 *AODf vs CDNC relationships for MODIS 6 (year 2008, upper left), for MODIS 5.1 (year 2007, upper right), for MODIS 6 (JJA of year 2008, lower left) and ATSR (JJA of year 2008, lower right). Matches were removed for mid-visible AODf values smaller than 0.05 (due to too poor signal to noise ratios) and larger than 0.25 (due to poor statistics). For individual AOD bins box-boundaries indicate the upper and lower quartiles, star symbols indicate averages and horizontal lines indicate median values. Logarithmic functions (displayed on top and illustrated by light blue lines) were fitted to the median bin values.*

The fits for the four scatterplots follow an expected log-normal fit as for a given AODf increase the associated CDNC increase will be smaller the higher the background AODf due to nuclei saturation. While there are differences to the pre-factors of the fitting functions, the multipliers for AODf (x) are identical (actually the same multiplier of 1000 applies well for all sensor data). The pre-factor cancels out when determining CDNC increase factors, because these increase factor are based on the ratio of two applications (CDNC [natur+anthrop] / CDNC [anthrop]). Thus, for the different satellite sensor data the derived CDNC factor increases from the different sensor data or data-subsets are basically identical.

Atmos. Chem. Phys. Discuss., https://doi.org/10.5194/acp-2018-949
Manuscript under review for journal Atmos. Chem. Phys.
Discussion started: 3 January 2019

Atmospheric Chemistry and Physics Discussions

The agreement for the (observational) fit functions for different satellite sensor data is quite in contrast to the diversity and to an (on average) much stronger Twomey effect in global modeling. These results are based on an analysis of output from nine global models with complex aerosol schemes that participated in the AeroCom (http://aerocom.met.no) indirect experiment. For the comparisons, the model simulated output for AODf and CDNC was sub-sampled at the same locations of the satellite matches. Scatter plots and associated fit functions between observational data (here MODIS coll.6) and the AeroCom model ensemble average are presented in Figure A3.

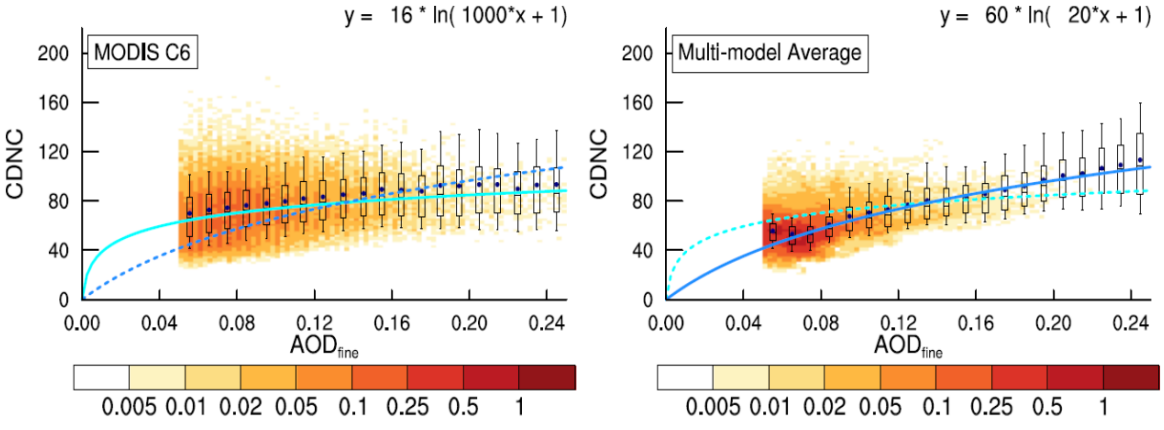

Figure A3 *AODf vs CDNC relationships as in figure A2 here based on a satellite retrieval (left, here MODIS 6) and on the AeroCom model ensemble average (right). Note the much steeper slope in global modeling (dark blue lines) which indicates a much stronger Twomey effect by global modeling than by satellite retrieval based 'observations' (light blue lines).*

The '+1' security value in the logarithmic fit (to avoid negative CDNC values) for the fine-mode AOD relationship to CDNC is raised '+3' to account for additional nuclei from coarse-mode aerosol. These contributions are particular important in fine-mode sparse regions over the southern oceans, to avoid potential overestimate for CDNC-factor increases. Thus:

CDNC, factor = ln (1000*AODf [natural +anthropogenic] +3) / ln (1000*AODf [natural] +3)

Applying today's total (natural and anthropogenic) AOD and natural AOD of MACv2, the CDNC increase factors due to anthropogenic aerosol are determined. And with the assumptions that the water content remains unchanged these CDNC increases are easily converted into droplet radius reductions.

radius, factor (%) = 100 / [(CDNC, factor)(1/3)]**

Atmos. Chem. Phys. Discuss., https://doi.org/10.5194/acp-2018-949
Manuscript under review for journal Atmos. Chem. Phys.
Discussion started: 3 January 2019

Atmospheric Chemistry and Physics Discussions

The seasonal averages for CDNC factor increases and water cloud droplet radius reductions (in %) associated with today's anthropogenic aerosol in the context of pre-existing aerosol are presented in Figure A4. There larger cloud droplet radius reductions are on the order of 10 %.

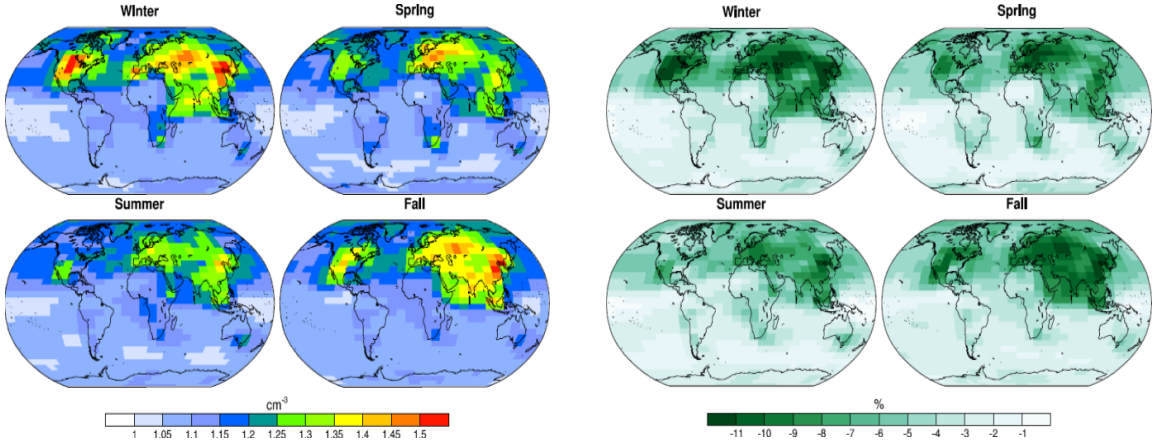

Figure A4 *seasonal CDNC factor increases (left) and associated droplet radius reductions in % (right) due to today's anthropogenic aerosol and the pre-industrial fine-mode background as defined by MACv2.*

Appendix B *MACv2 vs MACv1 and MACv2 vs MACv2-SP*

There are different MAC climatology flavors for aerosol optical properties in circulation. As impact differences are of interest, radiative effects at the TOA by today's anthropogenic AOD of the MACv2 climatology are compared to those when applying in off-line simulations (1) aerosol optical properties of the older MACv1 climatology (*Kinne et al., 2013*) or (2) aerosol optical properties of the plume approximation for anthropogenic AOD (*Stevens et al., 2017, Fiedler et al., 2018*) instead. Annual maps for direct aerosol effects at TOA are compared in Figure B1. Hereby, for the offline simulations with the MACv2-SP data with two different natural background conditions are assumed: one with a MACv1 natural background (M_SP_1) and one with a MACv2 natural background (M_SP_2).

Atmos. Chem. Phys. Discuss., https://doi.org/10.5194/acp-2018-949
Manuscript under review for journal Atmos. Chem. Phys.
Discussion started: 3 January 2019

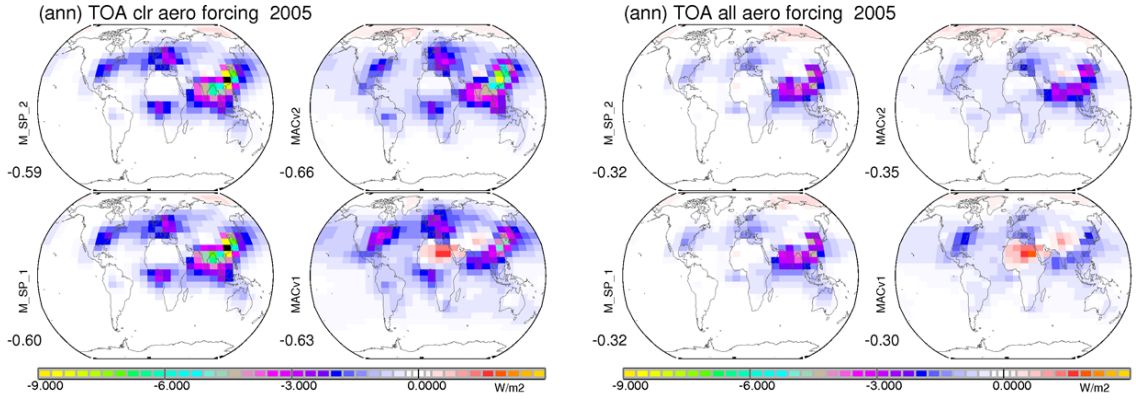

Figure B1. *annual maps for present-day aerosol direct radiative forcing in W/m2 at the TOA at clear-sky conditions (left block) and at all-sky conditions (right block) for MACv2-SP with MACv1 natural background (upper left) and with MACv2 natural background (lower left), for MACv2 (upper right) and MACv1 (lower right). Blue colors represent climate cooling and red colors indicate climate warming. Values below the labels indicate global averages.*

The MACv2-SP plume approximation yields MACv2 similar cooling patterns for present-day anthropogenic aerosol. However, MACv2-SP maxima are stronger (e.g. China) and weaker (e.g. South America). In the MACv2-SP plume approximation, contributions in remote regions are lower or completely missing, as individual plumes with limited spatial domains (even when combined) do not cover the entire globe. The impact by using different natural backgrounds in MACv2-SP (once using MACv1 natural aerosol and once using MACv2 natural aerosol) has only a small impact on the direct forcing. Globally averaged, both clear-sky and all-sky TOA cooling in MACv2-SP are ca 10% smaller than in MACv2, mainly as the mid-visible global average mid-visible anthropogenic AOD in MACv2-SP is only 0.028 compared to 0.031 in MACv2.

In the MACv1 climatology regional contributions for the direct forcing differ from MACv2 mainly due to differences in anthropogenic AOD regional strengths. MACv1 falsely allowed significant anthropogenic aerosols over the Sahara (associated with significant warming over the bright desert) along with too much anthropogenic aerosol over the US and Europe (for extra cooling). In MACv1 also anthropogenic aerosol over SE Asia is likely too low (for missing cooling). Globally averaged though, the direct forcing between MACv2 and MACv1 are similar as effects of a larger anthropogenic AOD of 0.040 in MACv1 (compared to 0.031 in MACv2) are compensated by significant warming over the Sahara.

Annual maps for today's indirect effects at the TOA by anthropogenic aerosol are compared in Figure B2. In all approaches, only indirect (Twomey) cooling effects at the TOA are considered and approximated based on the 'observed' satellite relationship between AODf and CDNC from MODIS and ATSR sensor data, as explained in Appendix A. The fit function is applied twice, once for natural AODf and once for total AODf (anthropogenic plus natural). Based on the logarithmic relationship a (local) CDNC increase factor was extracted. In MACv2 and MACv1 required AODf values (natural AODf and total AODf) are defined by the climatology. In MACv2-SP only the anthropogenic AODf is provided and

Atmos. Chem. Phys. Discuss., https://doi.org/10.5194/acp-2018-949
Manuscript under review for journal Atmos. Chem. Phys.
Discussion started: 3 January 2019

Atmospheric Chemistry and Physics Discussions

with assumptions to the natural AODf background (*Stevens et al., 2017*) already calculated CDNC increase factors are provided, so that the fit function application could not be tested.

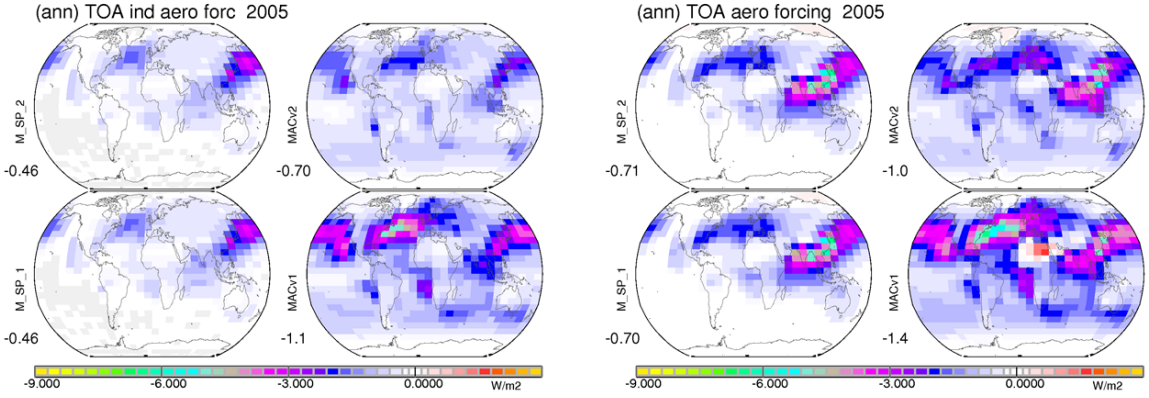

Figure B2. *annual maps for present-day aerosol indirect radiative forcing in W/m2 at the TOA at (left block) and for the combined direct and indirect radiative forcing (right block) for MACv2-SP with MACv1 natural background (upper left) and with MACv2 natural background (lower left), for MACv2 (upper right) and MACv1 (lower right). Values below the labels indicate global averages.*

In MACv2-SP the anthropogenic AOD has no global coverage so that in regions with no anthropogenic AOD no indirect aerosol effects are possible. This is the main reason that the globally averaged indirect TOA cooling in MACv2-SP is only ca 65% of the indirect TOA cooling by MACv2 - despite a much stronger MACv2-SP indirect response over the Pacific. For MACv1, in contrast, the indirect TOA cooling is ca 40% larger than in MACv2. The main reason here is a larger anthropogenic AODf comes at the expense of natural AODf. Both factors (more anthropogenic AODf, less natural AODf) lead to stronger CDNC increase factors and stronger indirect TOA cooling when applying the (retrieval based) fit function.

In Figure B2 also annual maps for the predicted combined (direct and indirect) TOA cooling impacts by today's anthropogenic AOD are compared. The MACv2 climatology suggests (when globally averaged) a combined present-day climate cooling near -1.0 W/m2, with the larger contribution from indirect effects. The associated uncertainty is estimated between -0.7 to -1.6 W/m2. To lower that range a more certain the pre-industrial reference and a better representation of indirect effect are needed.

The main argument for the upper bound -1.6W/m2 in climate cooling is that a larger fine-mode anthropogenic fine-mode fraction cannot be ruled out, although not quite as large as large as in MACv1, because the MACv1 anthropogenic fine-mode fraction based on AeroCom 1 emissions (*Dentener et al, 2006*) refers to year 1750. Still to illustrate anthropogenic uncertainty potential on present-day aerosol forcing, the MACv1 anthropogenic fine-mode fraction was applied with the MACv2 aerosol properties. As a result, the indirect effect increases to (from -0.65) to -1.1 W/m2 and the direct effect (from -.35) to -0.50 W/m2 for a combined -1.6W/m2 cooling. (A less negative -1.4 W/m2 with MACv1 aerosol

suffers from false direct warming over N.Africa.). While this upper bound of -1.6 W/m2 (due to the 1750 reference) is likely too negative, still a 15% potentially higher total AOD than prescribed by MACv2 aerosol should be considered (as shown with the use of ICAP ensemble background data in Figure 18).

The main argument for the lower bound of -0.7W/m2 in climate cooling is that the lower bound of the direct effect (which is better constrained than the indirect effect) is estimated at -0.2 W/m2 and of the indirect effect is estimated at -0.5 W/m2. A present-day direct effect cooling as low as -0.2 W/m2 cooling is possible with a higher than fine-mode anthropogenic fraction for BC. And for the present-day indirect effect, an even less negative than -0.5 W/m2 indirect MACv2-SP cooling does not qualify, as lower bound due to its incomplete global coverage for anthropogenic AOD.

Appendix C *monthly TOA forcing*

Monthly maps illustrate typical variations over the year for present-day aerosol radiative effects at the top of the atmosphere (TOA) for total aerosol in Figure C1 and anthropogenic aerosol in Figure C2.

Figure C1 presents for total aerosol the MACv2 associated radiative TOA effects. Monthly maps are presented for clear-sky (cloud-free) and all-sky conditions. Note that the effects in Figure C1 include infrared greenhouse effects by elevated coarse mode dust. For total aerosol, the global average effect is a climate cooling, despite intense climate warming over the Sahara, especially from April to September. The presented aerosol effects at all-sky conditions do not include anthropogenic indirect effects which would increase the TOA cooling by an additional -0.65W/m2.

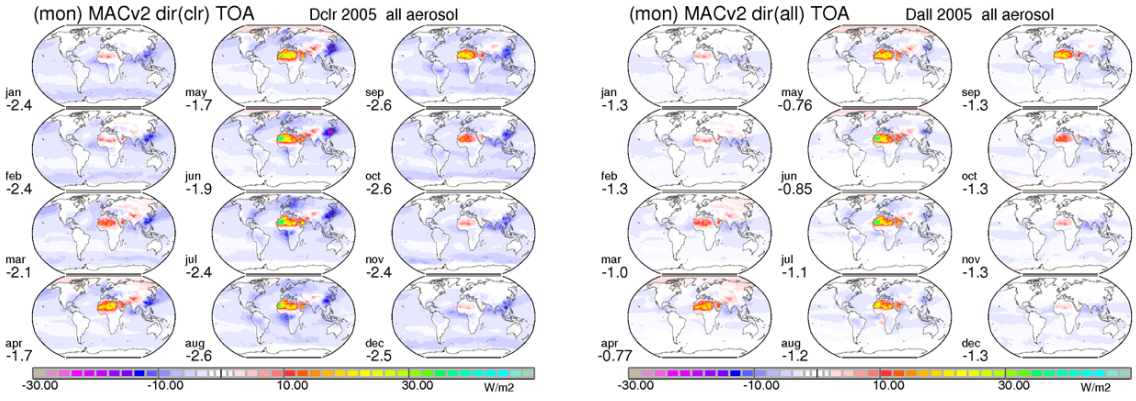

Figure C1. *monthly maps for the direct radiative forcing at the TOA by present-day total aerosol under clear-sky conditions (left block) and all-sky conditions (right block). Blue colors indicate climate cooling and red colors indicate climate warming. The infrared greenhouse effects by elevated coarse-mode mineral dust aerosol are included. Values below the labels indicate global averages.*

Atmos. Chem. Phys. Discuss., https://doi.org/10.5194/acp-2018-949
Manuscript under review for journal Atmos. Chem. Phys.
Discussion started: 3 January 2019

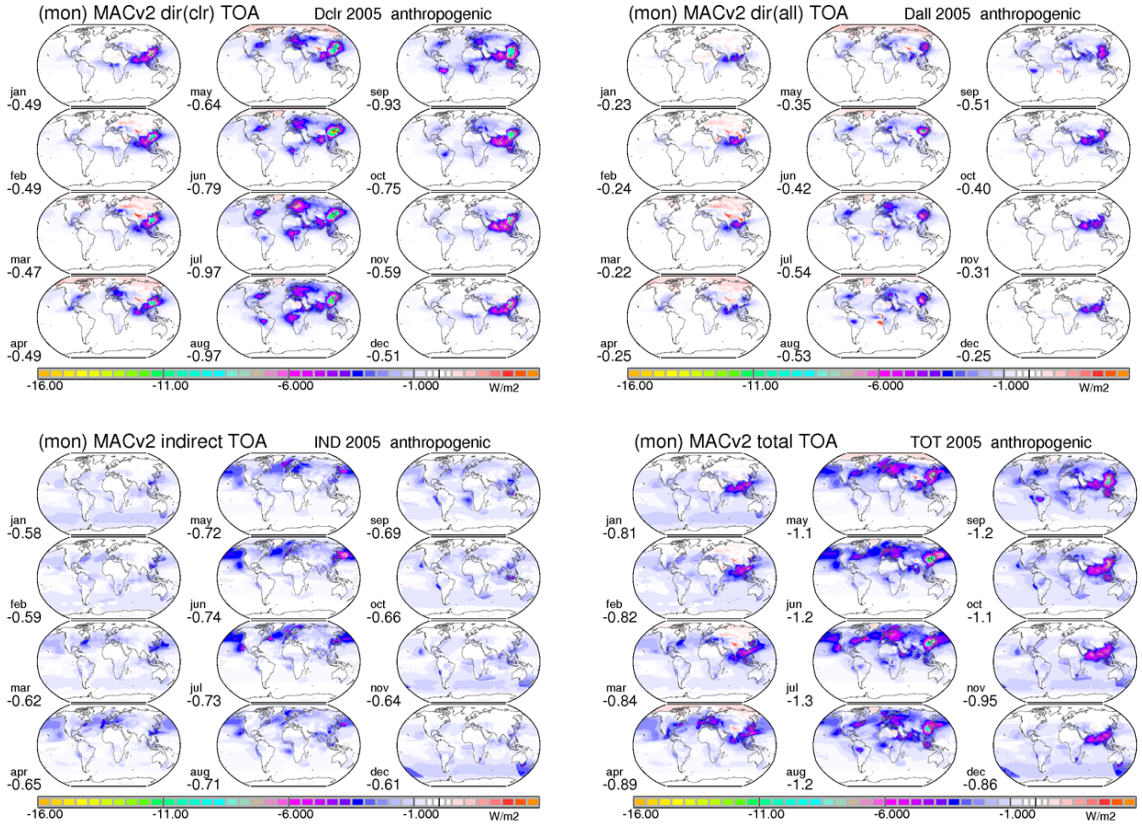

Figure C2. *monthly maps for radiative effects by present-day anthropogenic aerosol. Compared are direct radiative forcing by today's anthropogenic aerosol under clear-sky conditions (top, left block), direct radiative effects under all-sky conditions (top, right block), indirect effect (bottom, left block) and the combined (direct and indirect) effect (lower, right block). Blue colors indicate climate cooling and red colors indicate climate warming. Scales of all four blocks are identical to better compare contributions and seasonal dependencies. Values below the labels indicate global averages.*

Figure C2 presents for anthropogenic aerosol the MACv2 associated radiative TOA effects. Monthly maps are presented for the direct effect at cloud-free condition (Dclr) and all-sky conditions (direct forcing, Dall), for a (Twomey based) indirect forcing (IND) and for the combined (direct and indirect) forcing (TOT). In Figure C2 monthly maps were given the same scale for easier comparisons. They illustrate that for present-day aerosol forcing indirect contributions (IND) dominate over direct contributions (Dall) and that contributions are largest for the NH summer season with indirect effects globally slightly larger from May to August and direct effects globally largest from July to September.

Atmos. Chem. Phys. Discuss., https://doi.org/10.5194/acp-2018-949
Manuscript under review for journal Atmos. Chem. Phys.
Discussion started: 3 January 2019

Atmospheric Chemistry and Physics Discussions

Appendix D *monthly TOA direct forcing efficiencies*

Monthly maps for present-day TOA forcing efficiencies (per unit AOD) at clear-sky and all-sky conditions are shown for total aerosol in Figure D1 and for anthropogenic aerosol in Figure D2.

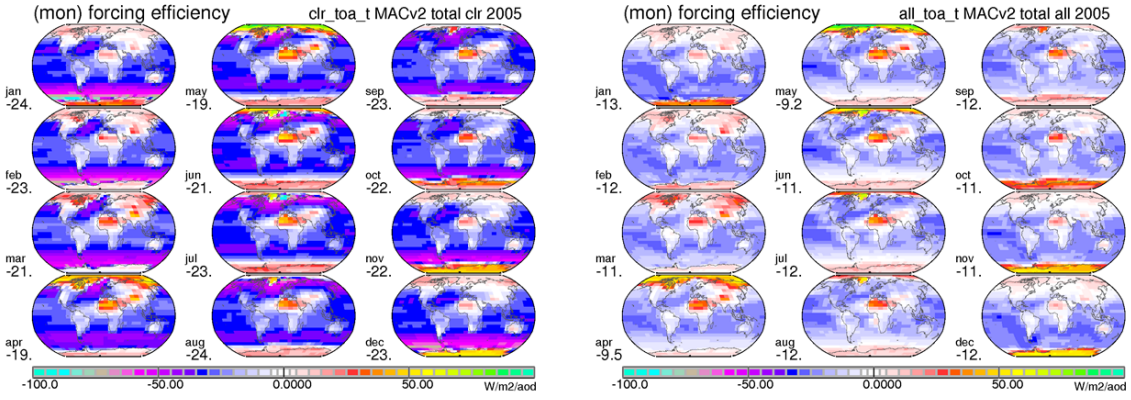

Figure D1. *monthly maps for the direct radiative forcing efficiency (per unit AOD) at the TOA by present-day total aerosol at clear-sky (left block) and all-sky conditions (right block). Blue colors indicate climate cooling potential and red colors warming potential. Values below the labels indicate global averages.*

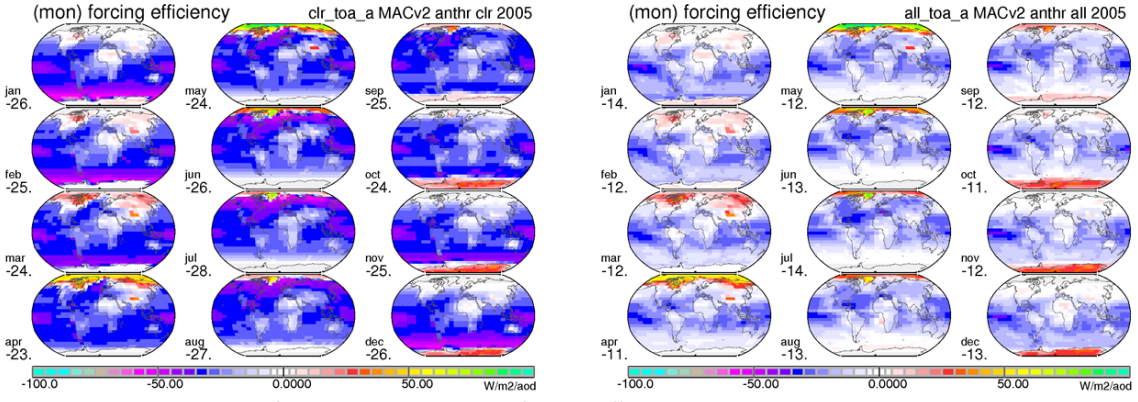

Figure D2. *monthly maps for the direct radiative forcing efficiency (per unit AOD) at the TOA by present-day anthropogenic aerosol at clear-sky (left block) and all-sky conditions (right block). Blue colors indicate climate cooling potential and red colors warming potential. Values indicate global averages.*

The global average forcing efficiencies (per unit AOD) for total and anthropogenic aerosol are similar and not only in their global averages (near -22 W/m2 at clear-sky conditions and near -11W/m2 at all-sky conditions) but also their spatial

Atmos. Chem. Phys. Discuss., https://doi.org/10.5194/acp-2018-949
Manuscript under review for journal Atmos. Chem. Phys.
Discussion started: 3 January 2019

Atmospheric Chemistry and Physics Discussions

patterns relatively stable over the year. Noteworthy is the switch in sign over Asia to positive values during the winter and spring due to snow cover and only for total aerosol the strong positive values over northern Africa.

Appendix E *component direct radiative effects*

With the attribution of optical and microphysical properties to (via size and refractive index) pre-defined aerosol types, type (or component) contributions are assigned such that their mixture is consistent with (local monthly data for) size-mode associated MACv2 mid-visible aerosol properties for AOD and AAOD. MACv2 component AOD assignments are presented in Figure F1.

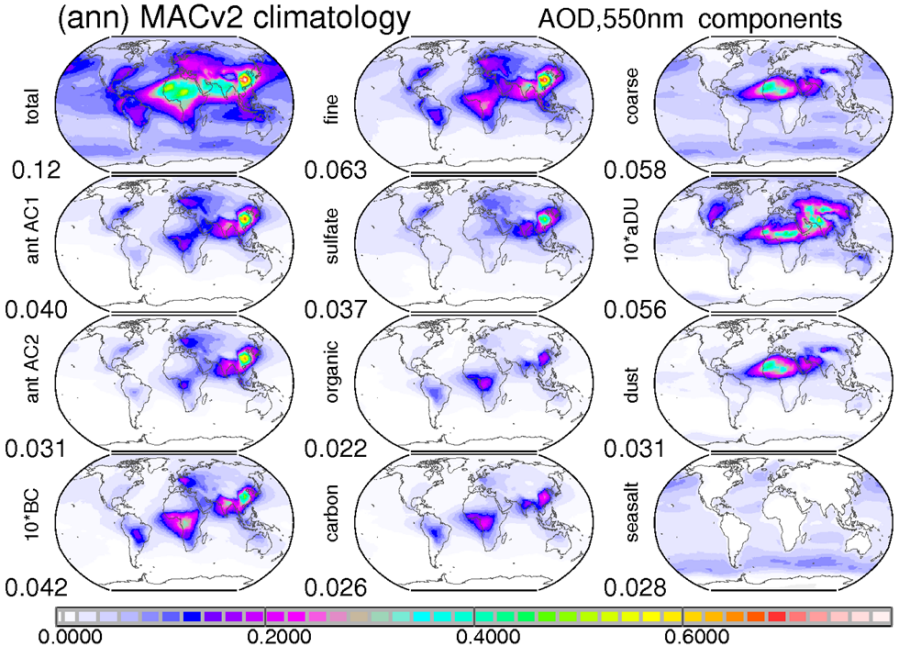

Figure E1 *annual average AOD maps for present-day tropospheric aerosol for total aerosol (top left) and contributions by fine-mode sizes (top center) and coarse-mode sizes (top right). In addition, consistent with mid-visible absorption data, component AOD values were assigned. Fine-mode AOD is divided into contributions by BC (soot, here multiplied by 10), OC (organics) and SU (where SU represents non-absorbing fine-mode). The coarse mode AOD is split into contributions by sea-salt and dust. In addition, annual AOD maps are presented for total carbon (OC+BC), for today's anthropogenic dust ('aDU', here multiplied by 10) and estimates for today's anthropogenic fine-mode AOD: 'ant AC2' of MACv2 and 'ant AC1' od MACv1. Values below the labels indicate global averages.*

Atmos. Chem. Phys. Discuss., https://doi.org/10.5194/acp-2018-949
Manuscript under review for journal Atmos. Chem. Phys.
Discussion started: 3 January 2019

The considered components are sulfate (SU - representing the fine-mode non-absorbing type), organic matter (OC), soot (BC) for the fine-mode and sea-salt (SS) and mineral dust (DU) for the coarse mode. Annual AOD maps of these components are compared in Figure E1. Hereby the size for SU and DU is allowed to vary, to satisfy MACv2 prescribed data for the fine-mode effective radius and the coarse mode absorption, respectively (*Kinne, 2018*). Below, in addition to the global averages of Figure 2, spatial distributions of present day direct aerosol radiative effects at TOA and surface, at clear-sky and all-sky conditions and for total impacts as well as impacts of contributions (such as anthropogenic, solar or infrared) are illustrated.

SU *(non-absorbing fine-mode)*

Annual maps for the cooling by present-day total and anthropogenic non-absorbing fine-mode aerosol (SU - to cover mainly impacts from sulfate and nitrate) are presented in Figure E2. Anthropogenic SU direct forcing (-.41 W/m2) is unevenly distributed and relative strong near sources. The anthropogenic impact at both TOA and surface is about half of today's total SU impact.

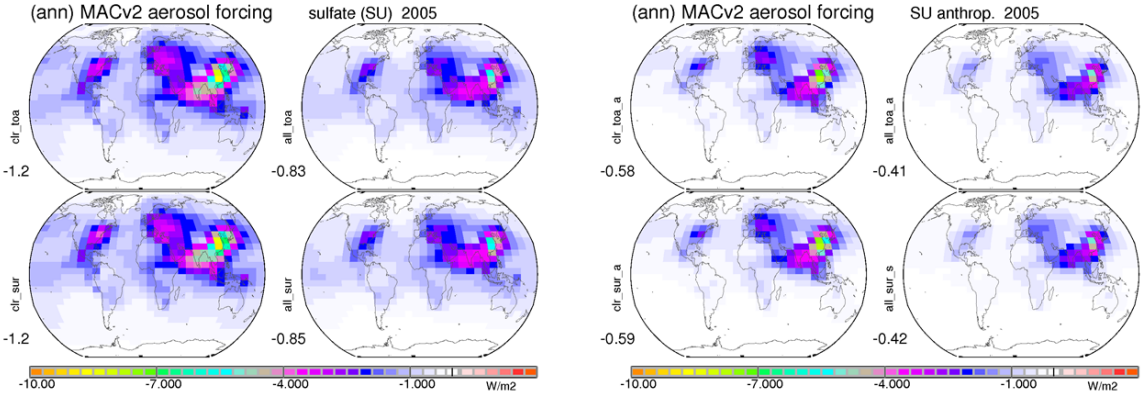

Figure E2. *maps of annual averages for present-day radiative effects of non-absorbing fine-mode aerosol (SU) at clear-sky (left) and all-sky conditions (right) at TOA (top) and surface (right). Total component impacts (left block) are compared to anthropogenic impacts (right block). Blue colors indicate a cooling and red colors a warming. Values below the labels are global averages.*

OC *(organic matter)*

Annual maps for cooling by present-day total and anthropogenic organic matter are presented in Figure E3. Anthropogenic OC direct forcing (-.22 W/m2) is unevenly distributed and relative strong near sources of pollution and wildfire regions. Due to solar absorption by OC, the cooling at the surface is larger than at TOA.

Atmos. Chem. Phys. Discuss., https://doi.org/10.5194/acp-2018-949
Manuscript under review for journal Atmos. Chem. Phys.
Discussion started: 3 January 2019

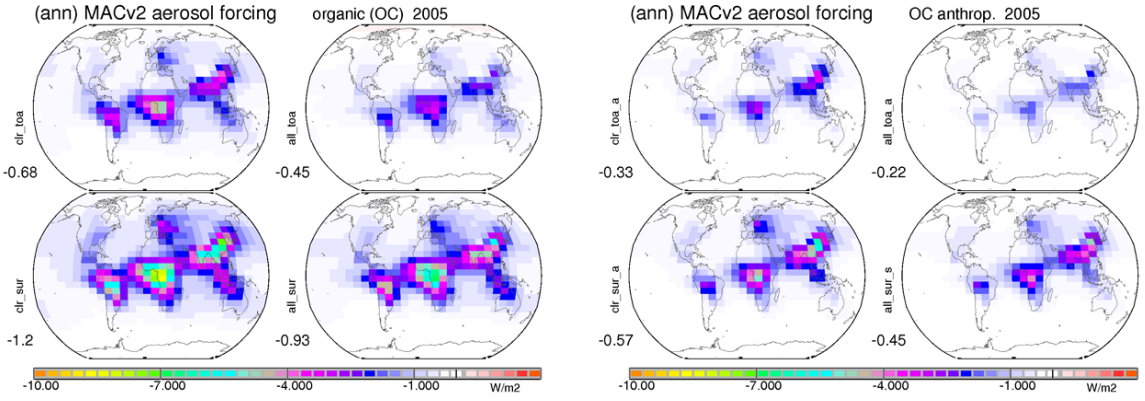

Figure E3. *maps of annual averages for present-day radiative effects of (fine-mode) organic carbon (OC) aerosol at clear-sky (left) and all-sky conditions (right) at TOA (top) and surface (right). Total component impacts (left block) are compared to anthropogenic impacts (right block). Blue colors indicate a cooling and red colors a warming. Values below the labels are global averages.*

BC (soot)

Annual maps for TOA warming and surface cooling by present-day total and anthropogenic soot (BC) are presented in Figure E4. Anthropogenic BC direct forcing (+.28 W/m2) is unevenly distributed with large values over wildfire region and in particular pollution regions. TOA warming by soot is larger with clouds (all-sky) due to dimming above lower clouds by absorbing aerosol.

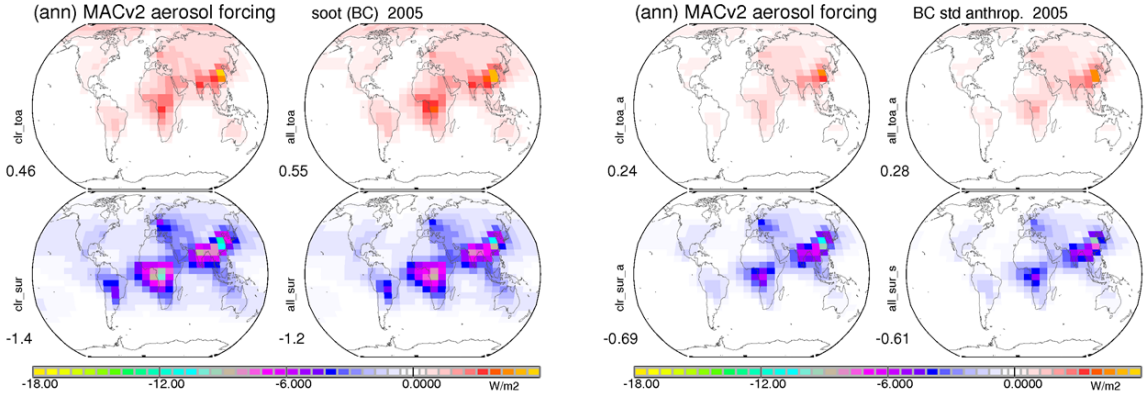

Figure E4. *maps of annual averages for present day radiative effects of (fine-mode) soot (BC) aerosol at clear-sky (left) and all-sky conditions (right) at TOA (top) and surface (right). Total component impacts (left block) are compared to anthropogenic impacts (right block). Blue colors indicate a cooling (at the surface) and red colors a warming (at TOA). Values below the labels are global averages.*

Atmos. Chem. Phys. Discuss., https://doi.org/10.5194/acp-2018-949
Manuscript under review for journal Atmos. Chem. Phys.
Discussion started: 3 January 2019

Atmospheric Chemistry and Physics Discussions

An alternate present-day BC anthropogenic direct forcing (+44 W/m2) is presented in Figure E5. Larger BC anthropogenic fractions (*Bond et al., 2013*) are assumed, which are larger than the fine-mode anthropogenic fraction near pollution source regions.

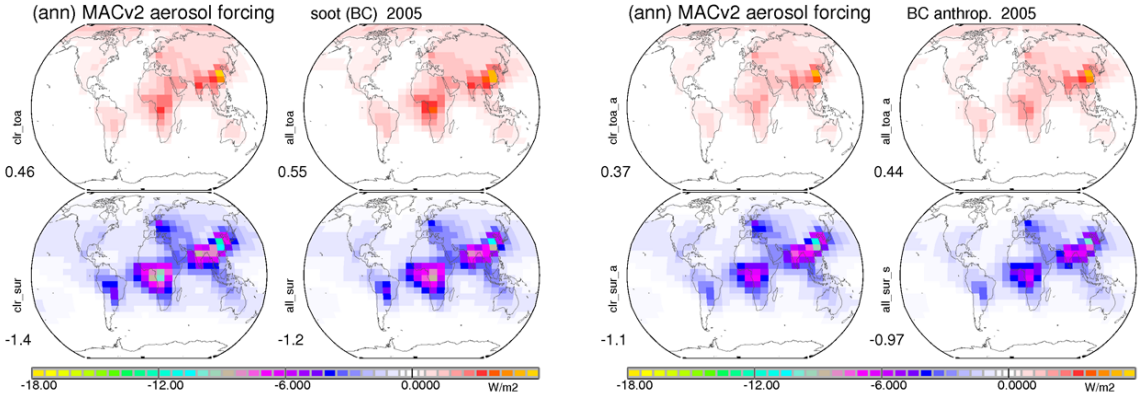

Figure E5. *maps of annual averages for present day radiative effects of (fine-mode) soot (BC) aerosol at clear-sky (left) and all-sky conditions (right) at TOA (top) and surface (right). Total component impacts (left block) are compared to an enhanced anthropogenic impact (right block). Blue colors indicate a cooling (at the surface) and red colors a warming (at TOA). Values below the labels are global averages.*

CA (carbon: OC+BC)

Annual maps for present-day direct radiative effects by total and anthropogenic carbon are presented in Figure E6. The anthropogenic carbon TOA response (+.05 W/m2) is almost climate neutral.

Atmos. Chem. Phys. Discuss., https://doi.org/10.5194/acp-2018-949
Manuscript under review for journal Atmos. Chem. Phys.
Discussion started: 3 January 2019

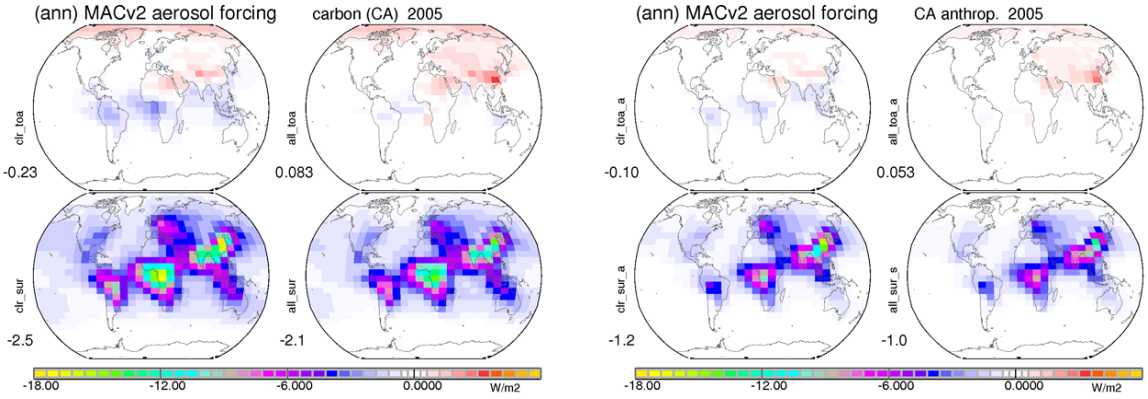

Figure E6. *maps of annual averages for present-day TOA radiative effects of (fine-mode) carbon (OC +BC) aerosol at clear-sky (left) and all-sky conditions (right) at TOA (top) and surface (right). Total component impacts (left block) are compared to anthropogenic impacts (right block). Blue colors indicate a cooling and red colors a warming. Values below the labels are global averages*

SS (sea-salt) and **DU** (mineral dust)

Annual maps for direct radiative effects by coarse mode (natural) components of sea-salt and mineral dust are compared in Figure E7. For sea-salt cooling maxima at TOA and surface are sharply reduced with the presence of clouds. For mineral dust the overall TOA warming is driven by a very strong warming over the Sahara. Individually contributing solar and infrared radiative effect maps are presented in Figure E8. Partially offsetting solar and infrared impacts are much stronger for a dominant solar cooling over oceans (at least at the surface) and a dominant infrared warming over continents.

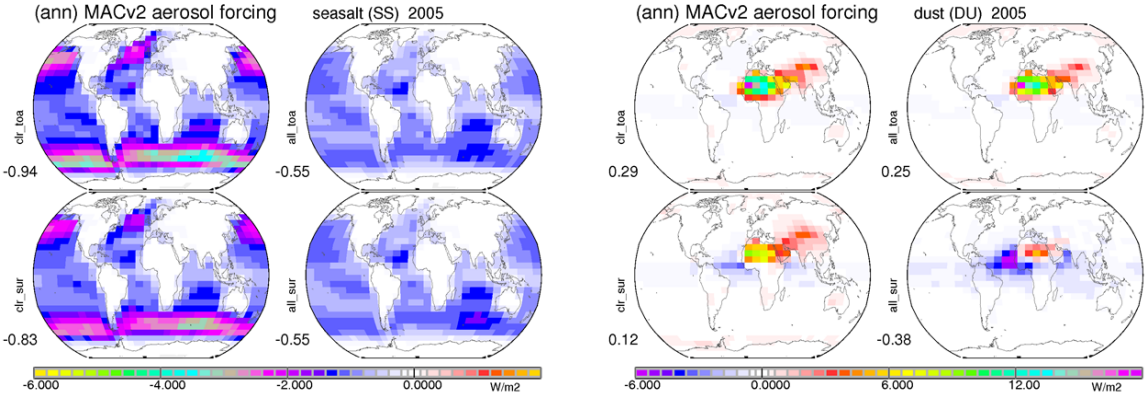

Figure E7. *maps of annual averages for present-day TOA radiative effects of coarse mode sea-salt (SS, left block) and coarse mode mineral dust (DU, right block) aerosol at clear-sky (left) and all-sky conditions (right) at TOA (top) and surface (bottom). Blue colors indicate a cooling and red to green colors show a warming. Values below the labels are global averages*

Atmos. Chem. Phys. Discuss., https://doi.org/10.5194/acp-2018-949
Manuscript under review for journal Atmos. Chem. Phys.
Discussion started: 3 January 2019

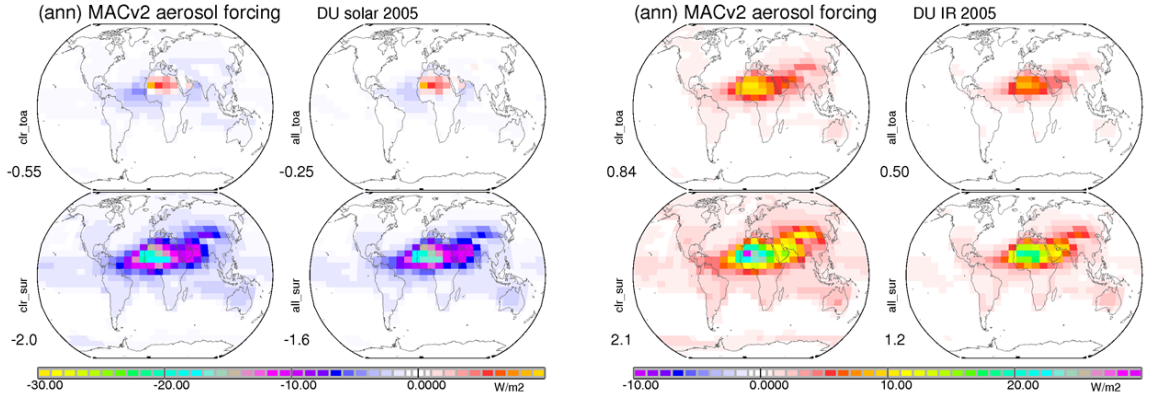

Figure E8. *maps of annual averages for present-day radiative effects of coarse mode mineral dust (DU) aerosol at clear-sky (left) and all-sky conditions (right) at TOA (top) and surface (right). Solar spectral dust impacts (left block) are compared to spectral infrared dust (right block). Blue colors indicate a cooling and red colors a warming. Values below the labels are global averages.*

Appendix F *aerosol indirect forcing sensitivity*

Aerosol indirect radiative effects show spatial distribution patterns, which may surprise, as the strongest impacts (e.g. mainly the increase in planetary albedo) are usually not at locations where anthropogenic AOD values are largest. The aerosol indirect effects or forcing is strongly influenced by environmental properties. A lower surface albedo, a high percentage of low altitude cloud cover without higher altitude clouds, a moderate optical depth for highest susceptibility and the available sun-hours during a day all favor a stronger indirect response. Based on these factors as summarized in Table F1 monthly indirect forcing potential maps are presented in Figure F1 along with monthly maps for MACv2 indirect forcing efficiency per unit anthropogenic AOD.

Atmos. Chem. Phys. Discuss., https://doi.org/10.5194/acp-2018-949
Manuscript under review for journal Atmos. Chem. Phys.
Discussion started: 3 January 2019

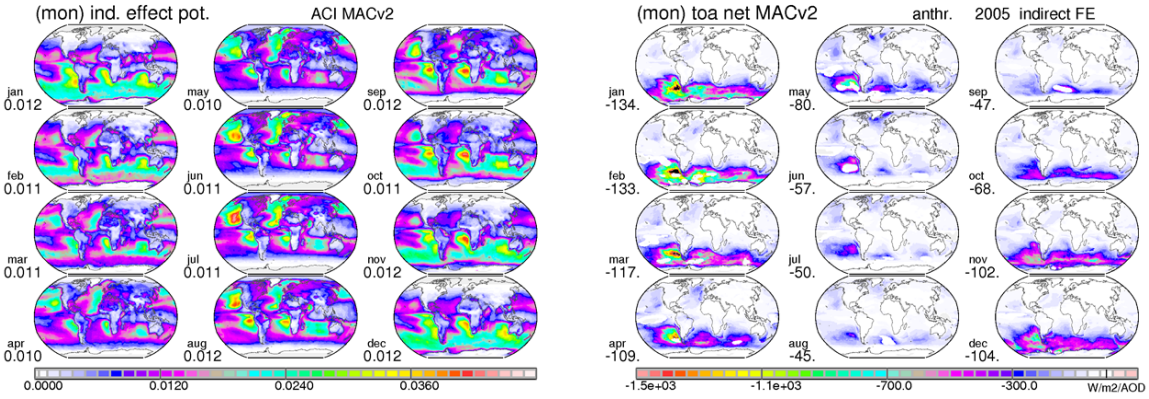

Figure F1 *monthly maps for environmental potential for aerosol indirect effects (left block) considering low cloud cover, reflection and susceptibility, surface albedo, sunshine hours and sun elevation and the indirect forcing efficiency (right block).*

Table F1*. assumed properties for the indirect environmental potential*

property	***assumptions***
cloud top temperature weight wei	>270K full impact (wei=1) <250K no impact (wei=0)
solar cloud reflection based R,cld	Rcld = (1 –exp(COT/(10+.35*COT)) COT-cloud optical depth
Susceptibility Scep	Scep = R,cld *(1.0 - R,cld)
Rcld, max is 0.67	0.67
consider the background factor B,f	B,f = 1.0-surf.albedo
low only cloud frequency F,low	F,low
scatter strength /sun-hours	sum{time(u0))*{1.0-abs(u0max-u0))**1.7}*exp(-0.025/u0**1.5)]} *with* u0max =0.25 +0.75*(1-exp(-0.22*cot**1.25)
environmental indirect potential	**= wei *Scep *.67 *B,f *F,low *sun**

The highest environmental potential for indirect effects is at oceanic stratocumulus regions off western continental coasts in the subtropics and at mid-to-high latitude oceanic regions during the sunnier spring and summer seasons. The aerosol indirect forcing efficiency (indirect forcing per unit anthropogenic AOD) displays a very high sensitivity over the southern oceans, where anthropogenic contributions are very low. As this high sensitivity is caused by the part of the logarithmic fit that is not well constrained by observations (see Appendix A) indirect effects are possibly overestimated over aerosol sparse regions, although absolute contributions to the MACv2 indirect forcing from these very clean regions are relatively small.

Atmos. Chem. Phys. Discuss., https://doi.org/10.5194/acp-2018-949
Manuscript under review for journal Atmos. Chem. Phys.
Discussion started: 3 January 2019

Atmospheric Chemistry and Physics Discussions

Appendix G *comparisons to other published aerosol direct radiative effects*

The present-day aerosol properties and associated direct radiative effects of MACv2 are here compared to complementary results from 'bottom-up' global modeling. More detail is provided by investigating component contributions in 'bottom-up' global modeling with assigned component data of the 'top-down' approach in MACv2.

First, mid-visible AOD and AAOD differences between a MACC reanalysis of assimilated MODIS AOD data in an ECMWF simulation (*Bellouin et al., 2013*) to MACv2 are investigated by comparing annual averages in Table G1.

Table G1*. comparison of properties for present-day mid-visible (550nm) AOD and AAOD data between the MACv2 aerosol climatology and the MACC reanalysis data.*

	AOD					**AAOD**			
	total	*DU*	*SS*	*fine*	*anthr*	*total*	*DU*	*fine*	*anthr*
MACv2	0.121	0.031	0.028	0.063	0.031	0.0072	0.0021	0.0051	0.0030
MACC	0.180	0.043	0.055	0.081	0.073	0.0080	0.0010	0.0070	0.0070

With the MODIS data-assimilation in MACC (*Bellouin et al., 2013*) the global average AOD is 50% higher. Thus is a likely overestimate as updated MISR retrievals (*M.Garay, personal communication*) and even the ICAP satellite assimilation ensemble (*Peng et al., 2013*) indicate and upper ceiling of 0.14 for the present-day global mid-visible AOD. The (for anthropogenic impacts relevant) fine-mode AOD MACC has a smaller relative contribution of the total AOD but is still larger than in MACv2. More of a concern is the large anthropogenic fraction of the fine-mode AOD in MACC, so that the present-day anthropogenic AOD is more than 2.5 times larger than in MACv2 – as all wildfires are incorrectly considered as anthropogenic in MACC. The MACC anthropogenic AOD has a slightly smaller absorption potential and the absorption potential of mineral dust is way too small, mainly due to a simplified dust size treatment in MACC. Differences in associated aerosol radiative effects are expected and shown in Table G2.

Table G2*. comparison of present-day aerosol associated aerosol radiative effects between the MACv2 aerosol climatology and the MACC reanalysis data (in W/m2)*

	clear-sky TOA solar direct radiative effect					**direct total forcing**	
	total	*DU*	*SS*	*fine*	*anthr*	*anthr*	*corrected*
MACv2	-3.5	-0.55	-0.91	-1.5	-0.70	-0.36	
MACC	-7.3	-1.6	-2.8	-2.8	-2.5	-0.70	-0.40

The MACC total aerosol present-day effect is too large, mainly because the total AOD is too large but also as the stronger cooling coarse-mode (missing mineral dust absorption/size) has a larger AOD fraction (too much seasalt).

The MACC aerosol present-day direct forcing of -0.7 W/m2 is too large as it includes wildfire contributions (*N. Bellouin, personal communication*). When removing those contributions the aerosol forcing is corrected downward to an agreeable -0.4 W/m2 cooling. Still, the contributing large reduction from clear-sky to an all-sky (from -2.5 to -0.7) in MACC raises proper cloud impact treatment questions.

Focusing on the fine-mode aerosol an its anthropogenic contributions the present-day aerosol direct forcing, along with component contributions of MACv2 was compared to 'bottom-up' ensemble averages of AeroCom (*Schulz et al., 2006*) and IPCC 5 modeling (*Myhre et al., 2013*) in Table G3.

Table G3*. comparisons of present-day aerosol direct radiative forcing (TOA, all-sky) in W/m2*

	total	**non-absorbing**		**absorbing**			
		SU	*NI*	*CA*	*BC*	*OC*	*SOA*
MACv2	-0.36 *(to -0.20)*	-0.41		+0.05 *(to +0.22)*	+0.28 *(to +0.44)*	-0.23	
Myhre avg	-0.32	-0.32	-0.08	+0.09	+0.18	-0.03	-0.06
Myhre med	-0.28	-0.32	-0.08	+0.13	+0.18	-0.03	-0.02
Schulz	-0.22	-0.32		+0.11	+0.25	-0.14	

MACv2 values with a much higher than fine-mode present-day anthropogenic soot (BC) fractions are in parenthesis

There is surprising good agreement for direct forcing estimates, even on a component basis. It is also shown, that if the prescribed fine-mode anthropogenic fraction in MACv2 is raised for soot (BC), then extra BC warming shifts the overall aerosol direct forcing to less negative values in MACv2. Thus, the possibility of a lower MACv2 direct effect cannot be ruled out. Here again, it is the limited understanding of the pre-industrial reference that introduces uncertainty.